Structural architecture, 3D modelling and target generation in the Lawn Hill Platform, Queensland

Project G14

Final Report
(July 2007)

Barry Murphy[1], Laurent Ailleres[2], Ben Jupp[2], Lawrence Leader[2], Terry Lees[2] and Indrajit Roy[3]

1 – University of Melbourne
2 – Monash University
3 – Geoscience Australia

bmurphy@unimelb.edu.au

Table of Contents

List of Figures

List of Tables

1 Summary

The ……unfinished business.

2 Introduction

A regional scale 3D architecture has been developed of the Lawn Hill platform (LHP) in NW Queensland. This seeks to constrain the distribution of large dimension faults and major stratigraphical units. An objective is to examine regional scale controls on the localisation of the world class Century zinc system which, in turn, may help in targeting areas of high exploration potential in the region. Aspects of this 3D map have been simplified, to derive a syn-mineralisation architecture, for input to numerical simulations of fluid flow and mixing environments (Zhang *et al.* 2006).

The 3D model covers an area of ~30,000 km^2, from the Fiery Creek Dome in the south to the Murphy inlier in the north (Figure 1). It includes the Lawn Hill 1:250 000 sheet, the northern part the Camooweal and the southern part of the Westmoreland sheets. A substantial body of data and previous research on the regional geology and geophysics impact on the 3D model. Geological mapping at 1:250,000 and 1:100,000 scales provide a well constrained geological template. Key sources of information are Sweet and Hutton's (1982) work on the 1:100,000 scale Lawn Hill sheet, Hutton and Sweet's (1982) review of the Lawn Hill platform and Andrew's (1998) work on the Upper McNamara Group of the Isa Superbasin. Regional scale basin and sequence stratigraphic analysis was undertaken by the NABRE project (Scott *et al*. 1998 and 2000; Southgate *et al*. 2000; Krassay *et al.* 2000 a, b; Bradshaw *et al.* 2000; Domagala *et al*. 2000) and integrated architectural studies by the AGCRC mainly in the southern parts of the region (Betts 1999, 2001; Betts *et al.* 1999 and 2006). Key basin analysis research through the AMIRA P552 project has been published (refs). The NWQMDR (2000) is an important resource and provides significant input to interpretation of the undercover geology, especially in the north-eastern sector of the study area (Figure 2). Geophysical data includes the Comalco seismic grid on the Westmoreland sheet, newly upgraded gravity data on the Lawn Hill sheet and MIM's open file aeromagnetic survey.

A summary of the regional geology is firstly outlined, followed by the potential field data sets and their interpretation. This provides a basis for extending the analysis into 3D modelling space, using the solid geology and cross sections as a key input. This model is supported by input from magnetotelluric data and preliminary interpretation of seismic data, which together provide key insights to the architecture of the region and the location of the Century deposit. An evaluation of the 2.5D structural architecture, focussing on fault intersections, is used as a template for identifying regions of higher exploration potential. The locations of such structural intersections and of potential host rock distributions within 3D model are then evaluated.

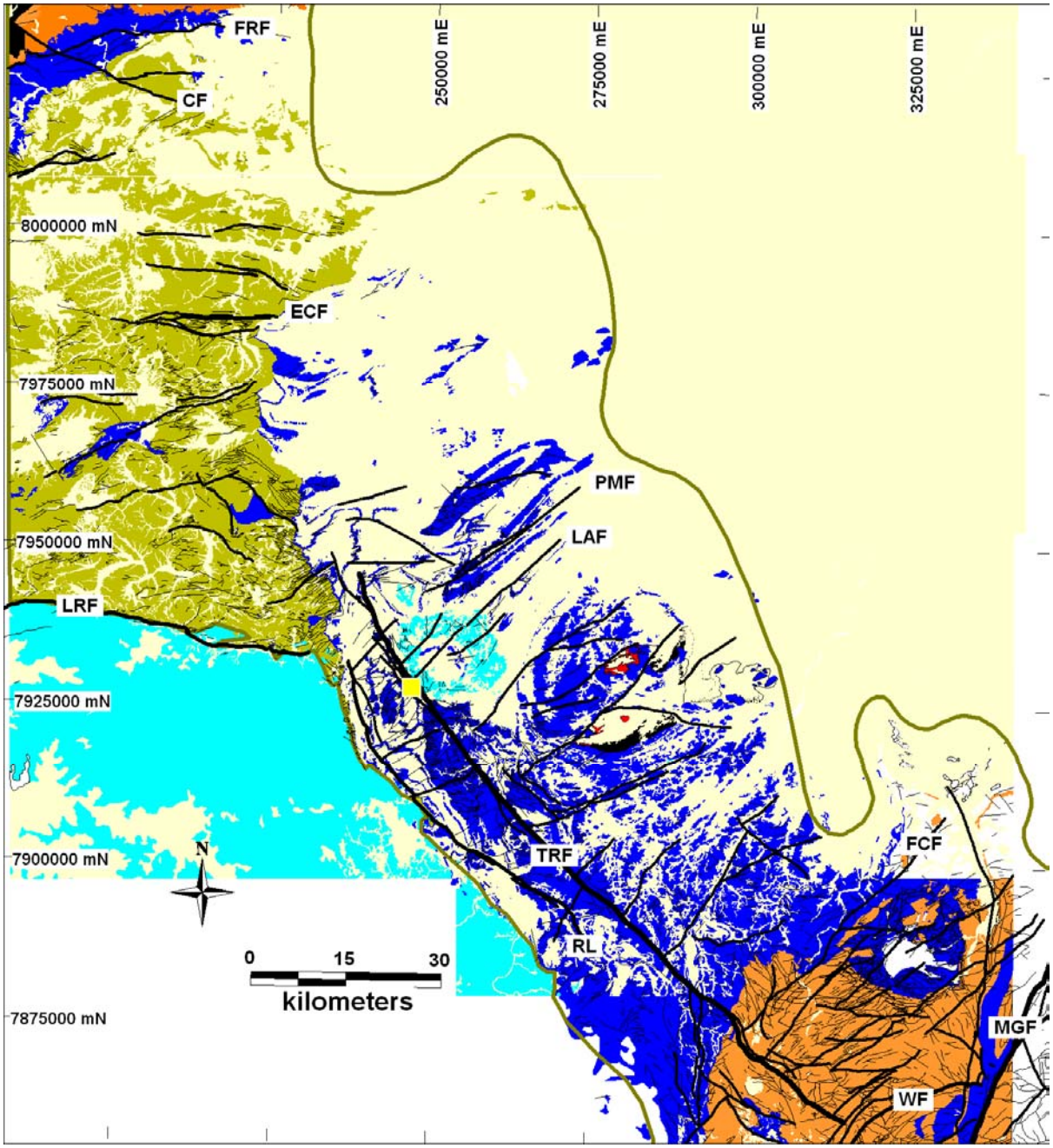

Figure 1: Simplified geological map showing distributions of the major rock units by Group.

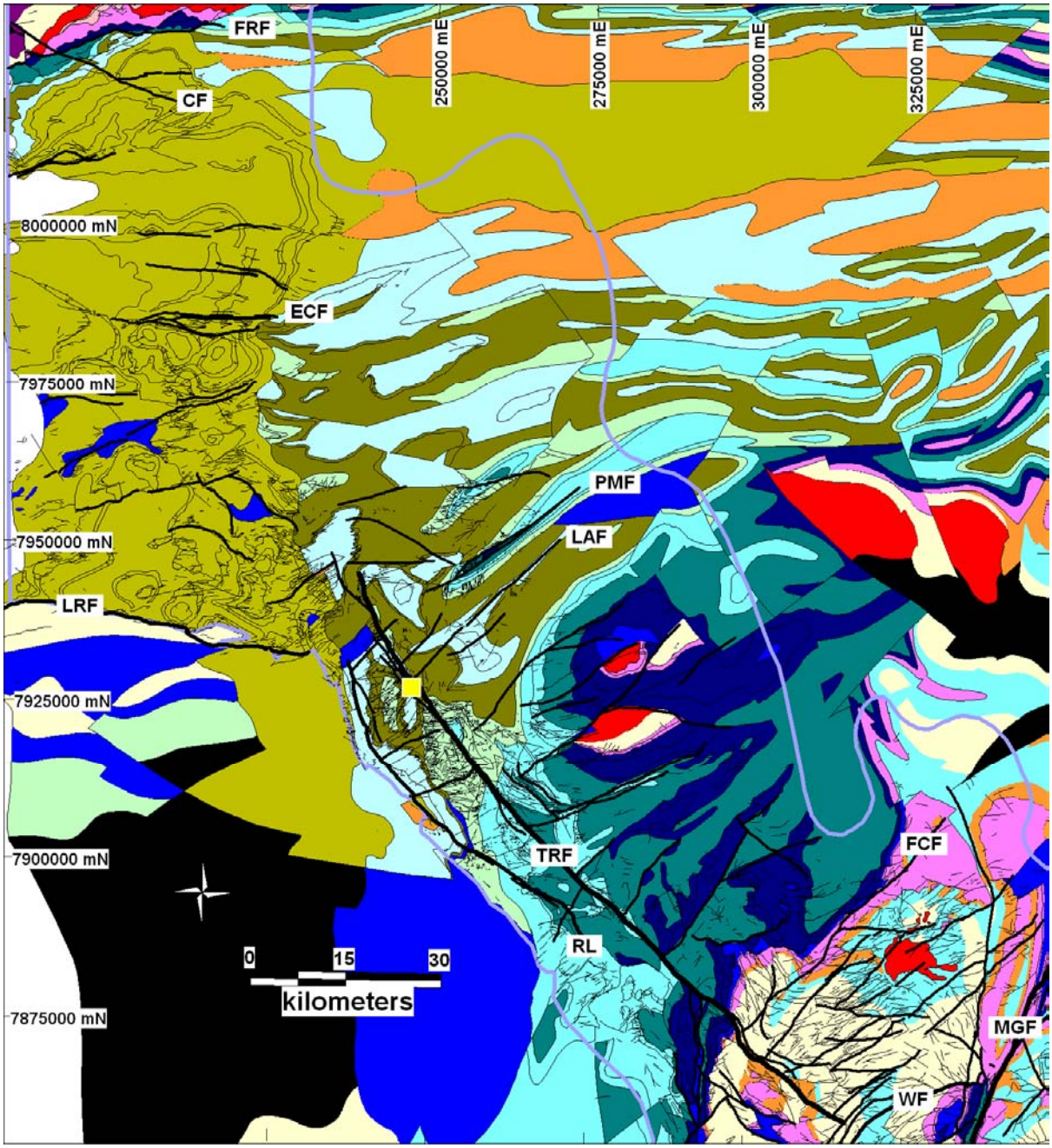

Figure 2: Regional geology and undercover interpretation based on NWQMPR Sequences

3 Regional Elements

INSERT TABLE 1: Stratigraphic Table

The main elements that comprise the stratigraphic pile and their relative distributions in outcropping areas are, from the base upwards:

- the Murphy Metamorphics (1890 Ma) exposed in two regions - in the Murphy Inlier to the north of the modelled area, and to the SW along the southern edge of the South Nicholson Basin in the Northern Territory (adjacent to the Cambrian Georgina Basin). These units are correlated with the Yaringa Metamorphics to the west and south of Mt Isa. This suggests a lateral continuity at depth of the basement and of its immediate cover sequence.
- the Cliffdale Volcanics (….Ma) outcrop in the Murphy inlier. These are correlated with the Leichhardt Volcanics (1865 Ma) in the Mt Isa region ("Cover Sequence 1")
- a plutonic event is recorded by the Yeldham Granite (1820 Ma) exposed in the core of the Kamarga Dome, near the centre of the modelled region, and by the Nicholson Granite Complex (1800 Ma) exposed in the Murphy inlier. Representatives of this in the Mt Isa region are the Kalkadoon and Ewen Batholiths and the Big Toby Granite (1800 Ma).

- the Wire Creek Sandstone of the Lower Tawallah Group exposed in the Murphy inlier. Interpreted as time equivalent to the Mt Guide Quartzite in the Haslingden Group ("Cover Sequence 2") of the Mt Isa Western Succession (Fig. 2).
- the Kamarga Volcanics (is there any age constraint?) exposed on the flanks of the Kamarga Dome (*post*-Yeldham Granite (cf. Sweet and Hutton 1982), and the Buddawadda Basalt Member in the Murphy inlier. Correlatives in the Western Succession are the Eastern Creek Volcanics.
- The Myally Subgroup, Quilalar Formation and Calvert Superbasin units of the Lower McNamara Group (Bigie Formation, Fiery Creek Volcanics and Surprise Creek Formation (and Lower Gunpowder Creek) all occur in the south of the region, in the Mt Oxide to Mt Isa regions. These are apparently absent, though non-deposition or erosion, at the Kamarga Dome where Isa Superbasin rests on Kamarga Volcanics and Yeldham Granite. Volcanics and sediments of the Carrara Range Group and Peters Creek Volcanics (1725 Ma) in the Murphy Inlier, and are correlated with the Fiery Creek Volcanics. (The Lower Fish River Formation in the Murphy inlier is included with this grouping?).
- The Weberra Granite (1698 Ma) in the core of the Weberra Dome in the Mt Oxide region.
- Isa Superbasin rocks of the Upper McNamara Group cover most of the Lawn Hill region, with the base at the Torpedo Creek/Warrina Park Quartzite. Lithostratigraphy and sequence stratigraphy are reasonably well constrained (Fig. 2). Correlative units in the Murphy inlier are the Fickling Group, where a significantly thinner sediment package is preserved. Seismic data south of the Murphy inlier shows a southward thickening of a sedimentary wedge and records a history of variable uplift and differential subsidence along the Murphy ridge (Scott *et al*. 1998). The Kamarga Dome also shows evidence of controlling sediment thickness and sediment supply during Isa Superbasin (Sweet and Hutton 1982). Krassay *et al.* (2000a) provide a palaeographic picture of this time interval showing some fault control of sediment thickness distributions (Figure 3).
- The South Nicholson Group with the base represented by the Constance Sandstone dominates the outcrop in the NW of the region.
- Cambrian Georgina Basin sediments, minor volcanics towards the base, occur in the SW of the modelled area. An outlier is preserved in the circular structure at Century. There is an intriguing relationship between the erosional edge of the Cambrian Georgina Basin and an inferred change in basement character beneath these covers rocks. Evidence that there may be pre-Barramundi basement at shallow levels comes from:
  1) the Murphy Metamorphics exposed in the Carrara Range, to the west, are overlain by the Cambrian sequence.
  2) the Yaringa Metamorphics to the west of Mt Isa are overlain by Isa Superbasin. This indicates a substantial unconformity or non-deposition of Calvert and Leichhardt rocks in the region.
- Mesozoic to Recent cover sediments dominate in the eastern parts of the modelled area.

The main structural elements are through-going faults and doubly plunging or dome and basin fold trends that are commonly spatially related to the fault structures. The largest of these, the Ploughed Mountain and Mount Caroline anticlines, south of the ECF, have been interpreted as "buttress folds" developed over basement-penetrating, rift-related faults that were re-activated during the Isan orogeny (Betts *et al*. 2004). The northern and central parts of the region are dominated by ENE-trending structures, with the Fish River Fault (FRF) along the southern flank of the Murphy inlier. Sub-parallel features to the south include the Mt Oscar (MOF) and Elizabeth Creek Faults (ECF). The dip direction of these ENE trending faults is mainly to NW (Betts *et al* 2004; cf. Scott et al. xxxx)

The Little Archie Creek Fault (LACF)
Archie Creek
TRF
RL
Wangunda
Fiery Creek, etccccc

The setting for the region is interpreted as comprising a regionally extensive pre-Barramundi metamorphic basement. This underwent repeated extension in a rift setting, with development of magmatic rocks (Leichardt Volcanics, Yeldham Granite, Eastern Creek Volcanics). Through differential tilting, subsidence and domal uplifts, the variable topography was partly infilled by the Calvert Superbasin, thinly developed on the Murphy Inlier Group, thickening southwards based on

seismic data, but absent from the Kamarga Dome, and becoming more extensive further south. The overlying Isa Superbasin sediments effectively blanket the region, with syn-sedimentary faulting resulting in sediment thickness variations. Variable uplift along the Murphy inlier suggests it acted as an intrabasinal topographic high within a broad region of intracontinental extension (Figure 4; Scott *et al*. 1998). There was a significant volcanic contribution to the detrital sediments in the Lawn Hill region, a source for which is not seen but is inferred beneath the Georgina Basin (Krassay *et al.* 2000b).

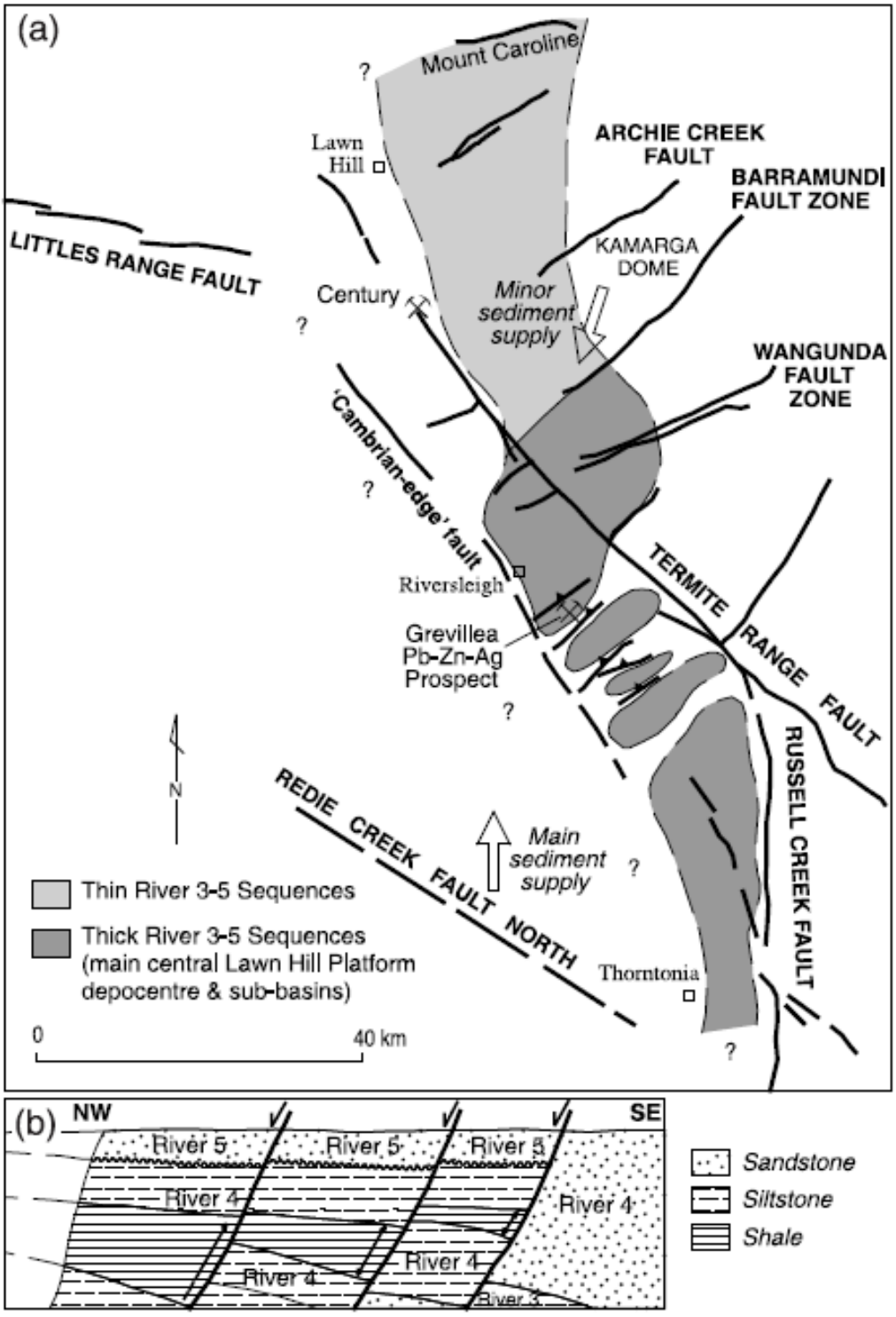

Figure 3: Palaeogeographic setting during Isa Superbasin times (from Krassay *et al.* 2000a)

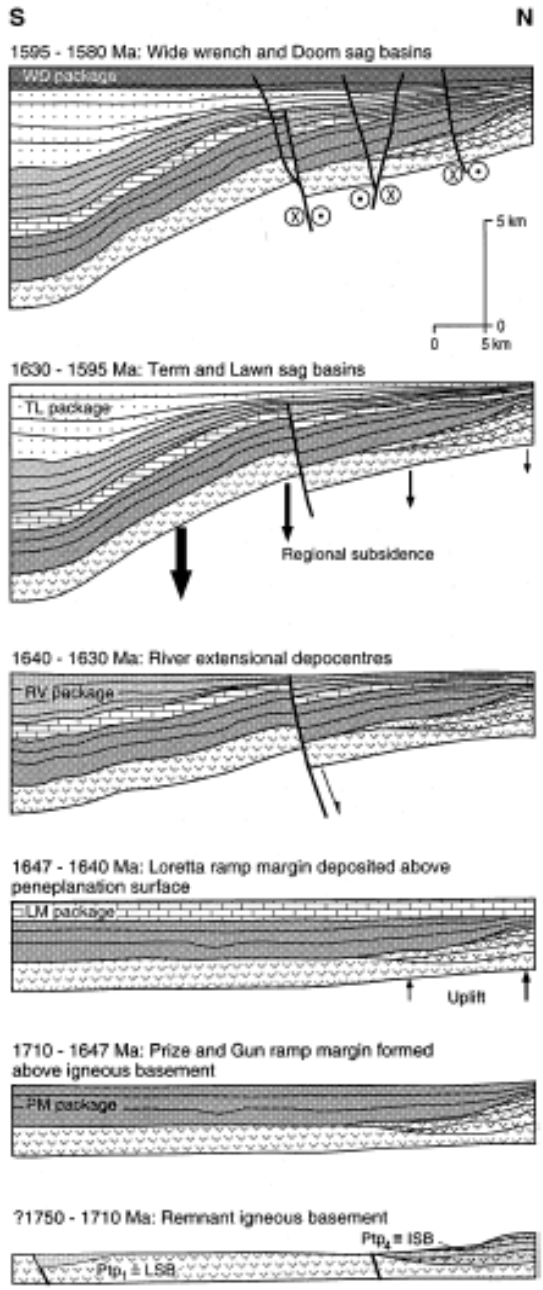

Figure 4: Interpreted subsidence history on the southern margin of the Murphy inlier (from Scott *et al.* 1998).

4 Methodology

The starting point for any 3D map is a solid geology base map and cross sections developed according to a standard legend. The base map was derived from the 1:100,000 and 1:250 000 published maps (Figure 1) and from the NWQMPR (Figure 2). More local scale data includes mapping by Andrews (xx) and a structural interpretation by ERA Maptec (King xx). The interpretation of potential field gradient data, detailed below, is a key input to this map and its 3D interpretation. This follows a similar methodology used by Murphy *et al.* (2006) in western Victoria. The bases of 6 units were traced out at 1:250 000 scale and extrapolated under cover (Figure 5). Five north-south and three east-west (BEN – any additional ones?; Figure 5) cross sections were drawn at 1:250 000 scale to 20km depth, with some forward modelling of the gravity and magnetic profiles undertaken to test the geometries; these are described (Section 6). Certain assumptions and caveats underpin the 3D model, including:

- The stratigraphic units are inferred to be widespread and have a pseudo-layer-cake distribution. In detail this assumption breaks down, as around the Kamarga and Fiery Creek Domes, and the model has attempted to represent these features where possible. In under-cover areas, however, such relationships cannot be readily determined.
- A relatively flat lying enveloping surface (sheet dip) is inferred. Within this are developed regional scale doubly plunging folds, such as the large (10's km strike length) dimension Ploughed Mountain and Mt Caroline anticlines. These are interpreted as fault-related folds developed above deeper level faults (Betts *et al.* 2004). It is generally not possible to represent smaller scale fold structures in the regional 3D model.
- Large dimension faults are important elements of the model. These are generally well represented in the mapped geology, but in under-cover areas a reliance on interpretation of potential field data is critical. In order to minimise the ambiguity and maximise the value of the potential field data, an automated edge detection routine (called "worms") was used to capture and assess the distribution of gradients in the region. These data sets are presented below. From this, an interpretation of the near-surface fault architecture is developed. This becomes a basis for extracting the large dimension faults that are then represented in the 3D model. The dip and depth extent of faults are key uncertainties. The wormed potential field data provide some constraints on these geometries. Additional important constraints are from magnetotelluric and seismic data, referred to respectively below.
- A last point is the choice of 3D modelling software. In this instance, "Geomodeller", subsequently named "3DWEG", was used as it showed potential to be effective in regions of relatively low geological complexity. The program allows for interpolation through areas of sparse control. As the software was still in development stages, however, a number of issues delayed production of the model.

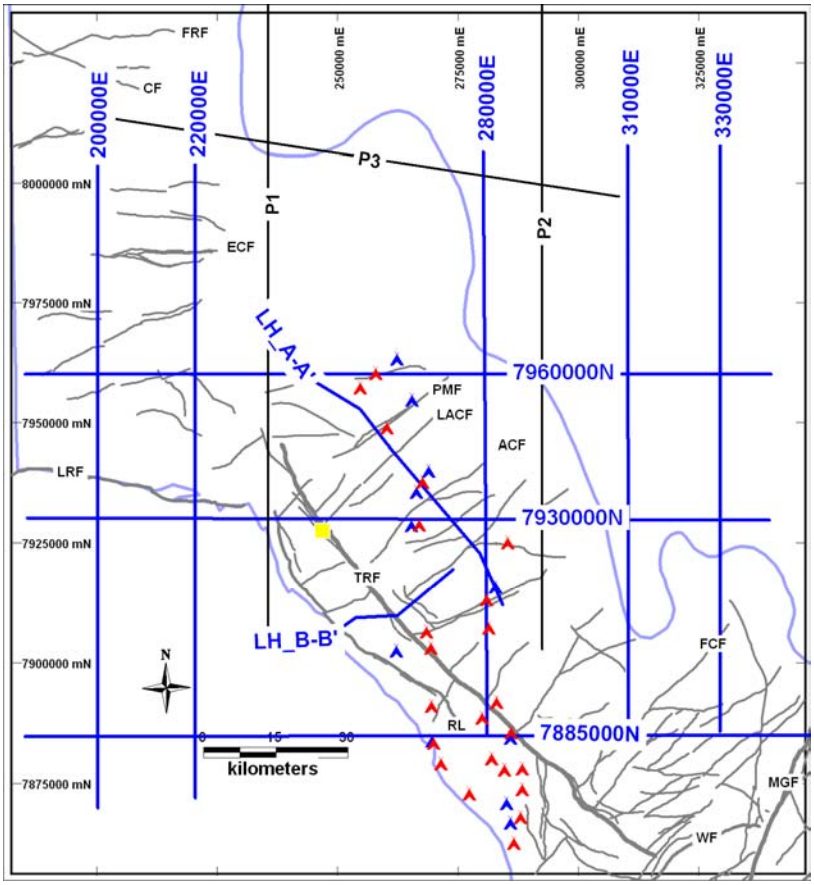

Figure 5: Locations of geological cross sections and forward modelled profiles. AMIRA P552 Profiles (P1, P2, P3). Tent symbols are measured sections from Sweet and Hutton (1982; red = Shady Bore; blue = Riversleigh Siltstone). And TOPO Z?? omit fault names…show MT and seismic profiles, inc westmoreland

4.1 Faults

One function of a 3D geological map is to portray the dimensions and shapes of the major, laterally persistent faults. In this regard, strike length may be a loose proxy for penetrative faults. To illustrate this, faults lines have been processed to show strike length attributes (Figure 6). Lines contained in such data sets are highly segmented in their native digital form, and to provide a more meaningful picture of the fault population, the line elements were concatenated, i.e. contiguous lines were joined together. There is subjectivity with establishing linkages between structures, and reference is made to continuity in strike direction and to solid geology constraints. Naturally, some faults die or are displaced; Ockham's Razor ("entities should not be multiplied unnecessarily") is employed in the interpretation routine which seeks to maintain line continuity rather than segmentation (as per the original data).

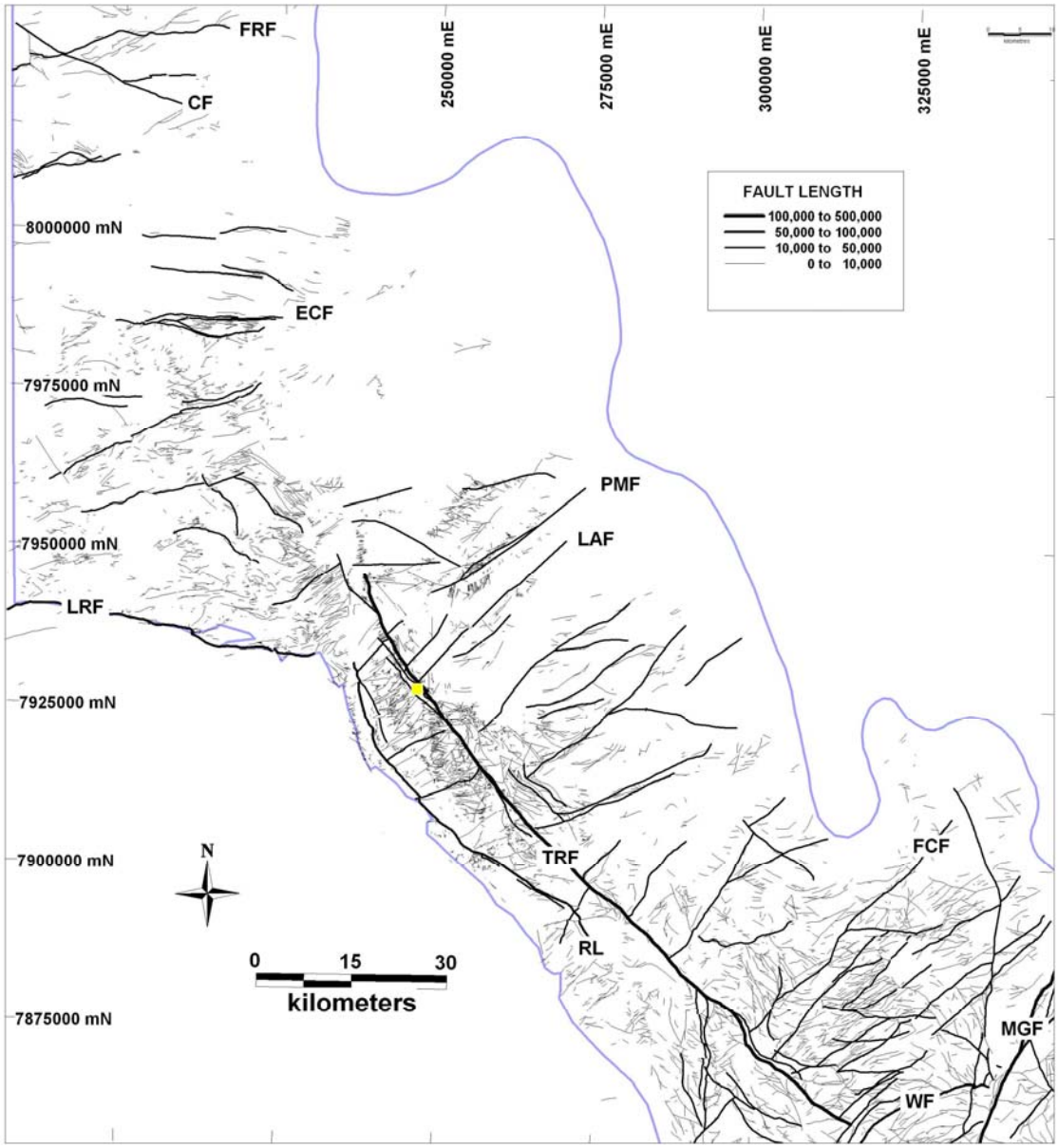

Figure 6: Mapped faults ranked by length (m). Abbreviated fault names: ACF = Archie Creek, BF = Barramundi, CF = Calvert, ECF = Elizabeth Creek, FCF = Fiery Creek, FRF = Fish River, LACF = Little Archie Creek, LRF = Little Range, MGF = Mt Gordon, RCF = Russell Creek, RL = Riverlseigh Lineament, TRF = Termite Range, WF= Weberra, WaF = Wangunda.

4.2 Potential Field Gradients

Traditional interpretation of potential field data requires the interpreter to trace a boundary line between contrasting bodies to represent a geological entity (e.g. fault, intrusive, stratigraphic contact). As one person's boundary line will differ from that of another's, this inherent variability impacts on reliability and repeatability of the interpretation. In order to reduce ambiguity, the analysis used here employs a comparatively new technique called multiscale wavelet edges (aka "worms") to trace the positions of gradients in the potential field. This is an automated edge detection routine, developed by CSIRO and Fractal Graphics (Hornby et al. 1999; Archibald et al. 1999). It is applied to gravity and aeromagnetic data over multiple (above-ground) height levels of upward continuation (u.c.) from which the positions of maximum gradient are detected. These gradients range across a spectrum of values from high frequency-short wavelength ("fine scale" at low u.c. levels) to low frequency-long wavelength signals ("coarse scale" at high u.c. levels). As an automated technique, it makes for a more robust interpretation.

The focus here is gradients in the potential field, rather than the causative bodies themselves. Multiscale wavelet processing detects gradients (and their amplitudes), but does not inform us of the distribution of high and low signatures that create these gradients. The "worm" data consist of points that represent the position of maximum gradient at a specified u.c. height which, when viewed at appropriate scales (i.e. over multiple height levels), appear to coalesce as clouds of points that are termed "worm sheets" (Figure 7). The shape of a worm sheet can inform the interpreter about the source boundary, its dip and relative depth. (Holden *et al.* 2000). Importantly, the height extent of a worm sheet may relate to the source depth, with a rule of thumb being that the u.c. height (Z) is approximately twice the source depth (i.e. a worm gradient at 10km height may relate to a geological edge at 5km depth). Hence, long wavelength-low frequency worms may indicate deep crustal boundaries. Gravity data are generally more reliable than aeromagnetics in this regard. A caveat is that such interpretations carry considerable uncertainty when made in isolation, and need to be evaluated on a case-by-case basis, using other independent data where available (e.g. geological maps, seismic data). In addition, the worm data has an amplitude value (W) that is a measure of the relative contrast across the boundary, i.e. a high amplitude value indicates juxtaposition of strongly contrasting bodies. Amplitude variations in a worm sheet may be a sensitive indicator of alteration processes, such as magnetite creation or destruction.

The worming process offers significant advantages over conventional methods in that it captures virtually all of the visually observed gradients across multiple scales. In doing so, however, it generates enormous data sets that can be cumbersome to manage and manipulate, whether on 3D or 2D platforms. A systematic analysis of such data becomes a signal processing issue and proprietary software, Geoscope, was developed through the pmd*CRC to enable more efficient post-processing of the data (Murphy and Russell-Head 2006; see TWiki New Tools web page). This provides bitmaps of worm data coloured by height (Z) and amplitude (W). A numerical (nearest-neighbour algorithm) process of migration from higher to lower u.c. levels yields images of height-weighted points (Zwt); this reflects the height level of a gradient at a selected level, effectively a 2.5D representation of the 3D data. These points are converted to vector lines with parameters of length, height, trend and straightness. Such outputs provide a quantitative basis for interpretation of what is a mixed population of gradients from a variety of geological sources. At one end of the spectrum are long, straight and high level-long wavelength gradients, and typically relate to penetrative faults and/or boundaries of major stratigraphical or intrusive units. At the other end of the spectrum, amidst the noise, are short, highly curved (or enclosed) gradients, such as due to shallow, depth limited intrusives. Visual inspection of naturally occurring worm data often reveals linear breaks and offsets of gradient traces, and these may be interpreted as cross-faults which have no density contrast across them. The interpretation seeks to capture such elements and incorporate them with the digital processing.

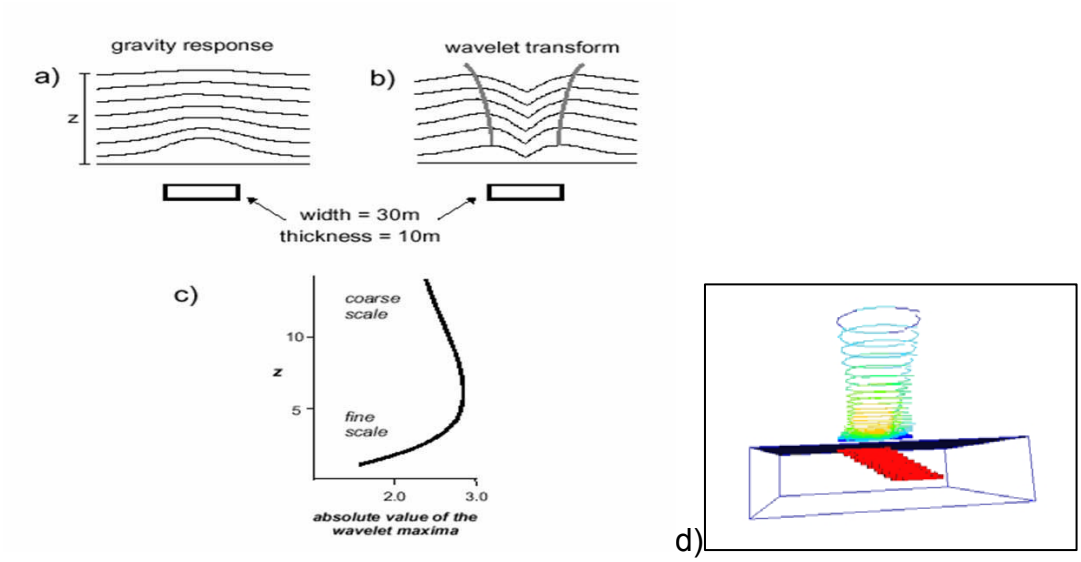

Figure 7: Multiscale wavelets: a) vertical profile of a buried body and its gravity response decaying across upward continued levels (Z), b) wavelet transform to determine worm points of maximum gradient at each height level, joined across levels as a worm sheet, c) plot of amplitude (W) against height (Z), from fine to coarse scale, reaching maxima at height level related to depth of body, d) perspective view of synthetic model of dipping cylinder (red) with above ground, upward continued levels defining a worm sheet (coloured by amplitude); shape of worm sheet mirrors dip of cylinder in lower u.c. levels. (Hornby *et al.* 1999; Archibald *et al.* 1999)

4.2.1 Regional Gravity

A Bouguer image from newly released data collected on ~3km station spacing is shown (Figure 8). An extensive broad low characterises the south-western region which underlies the Georgina Basin but extends northwards beyond the outcrop of the Cambrian. A regional high is seen in the eastern under-cover region and this broadly describes an arcuate shape that merges with the east-west trending basement-related high in the north, the Murphy Ridge (ref?). A number of linear trends are seen in the image, and the mapped faults in places correlate with changes in Bouguer intensity. To assess this further, the gravity data was upward continued using multiscale wavelet processing (by Geoscience Australia algorithms) from 500 m to 104 km height (Figure 9). The resultant gradient image displays higher level gradients as warmer worm colours. Although a range of geological sources is represented, several of the major gradients appear to correlate with the trend and positions of mapped faults.

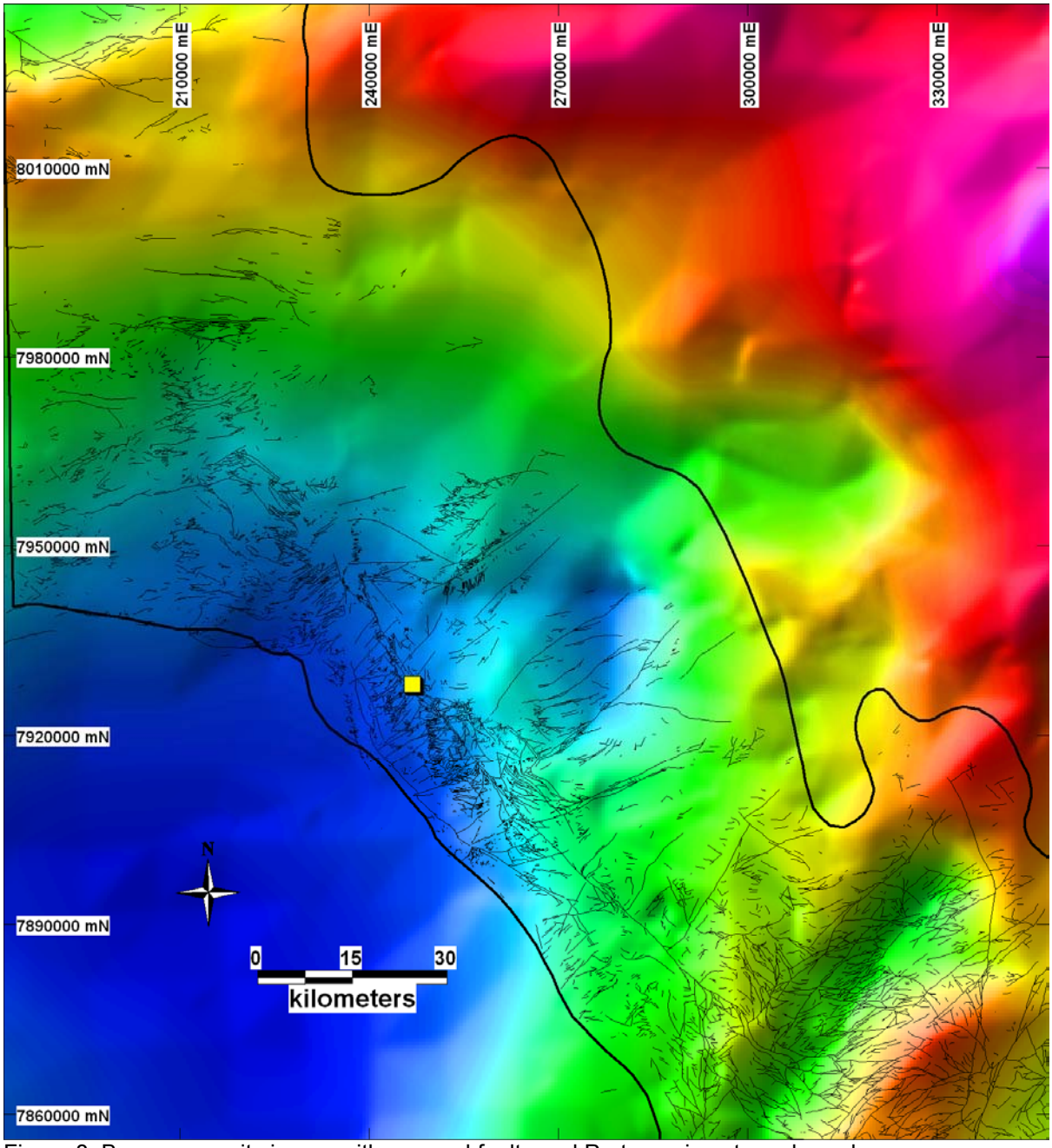

Figure 8: Bouguer gravity image with mapped faults and Proterozoic outcrop boundary.

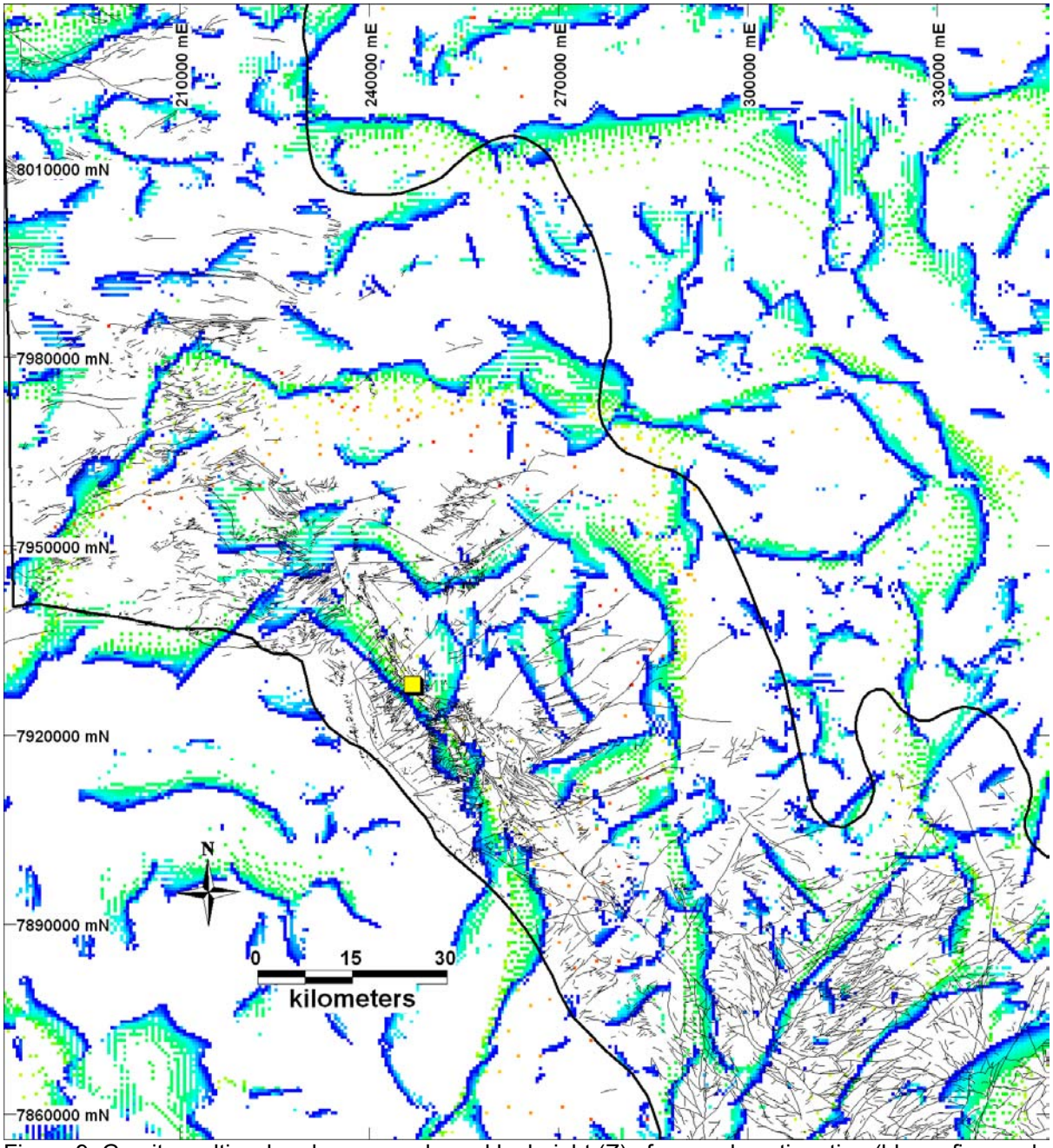

Figure 9: Gravity multiscale edge map coloured by height (Z) of upward continuation (blue = fine scale, red/orange = coarse scale) with mapped faults and Proterozoic outcrop boundary.

4.2.2 Regional Aeromagnetics

The aeromagnetic data show a range of signatures in the Total Magnetic Intensity image (Figure 10). Broad domains of relatively coherent signature are generally bounded by major faults. MIM's' open file aeromagnetic data at 400m line spacing was used for the worming process using Fractal Graphics multiscale edge algorithms, from which 32 levels of upward continuation from 200m to 30km height were derived (Murphy 2002). Two types of processed worms were used: Max (maximum gradient; the Figure 11) and EFVD (effective first vertical derivative; Figure 12); the latter provides a more complete representation of near surface gradient points. A second set of worms was generated for the region north of the MIM survey, in the Mornington region (from 8000000N). This was processed using Geoscience Australia's algorithm, over 33 levels of upward continuation from 300 m to 45 km height.

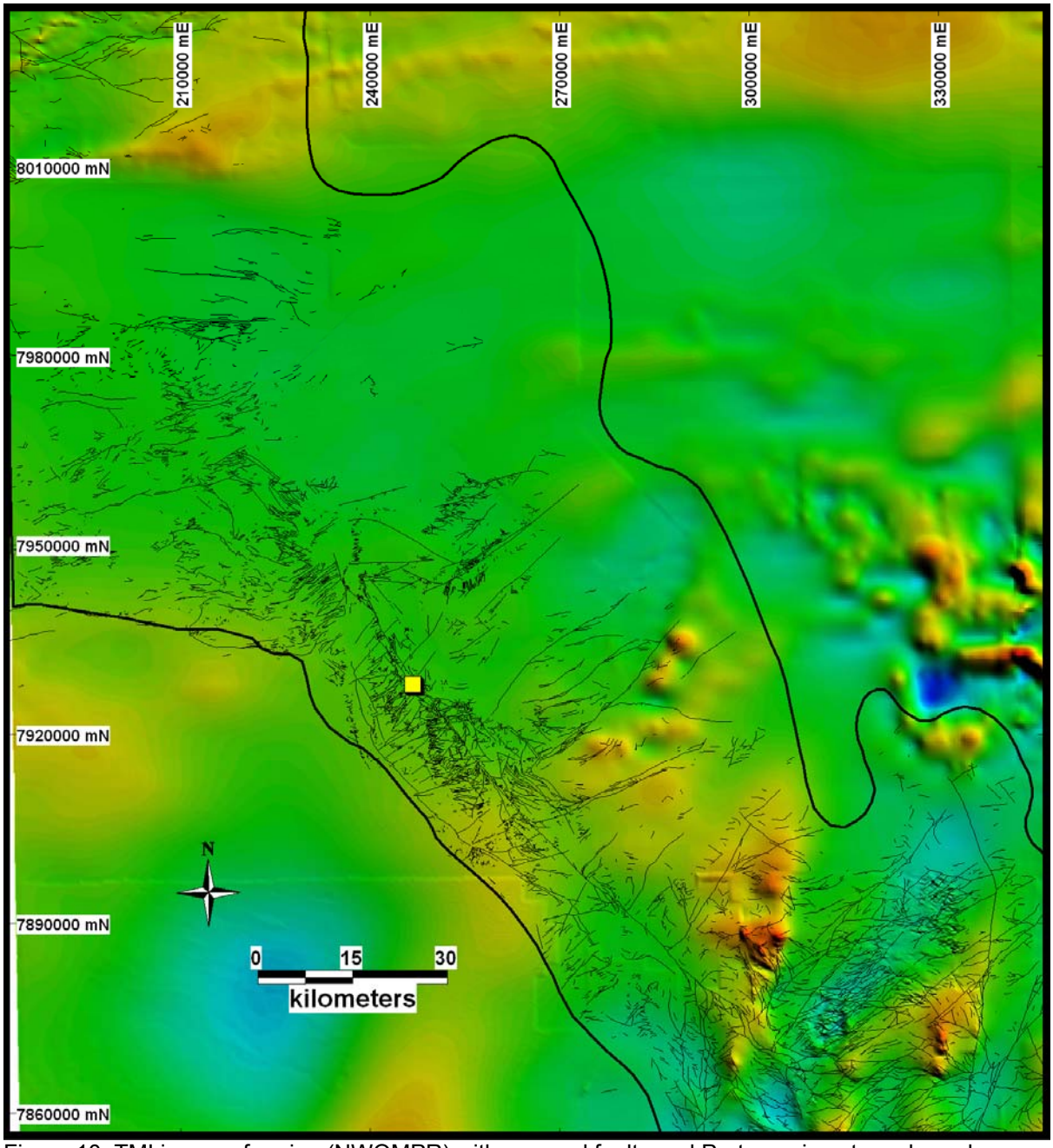

Figure 10: TMI image of region (NWQMPR) with mapped faults and Proterozoic outcrop boundary.

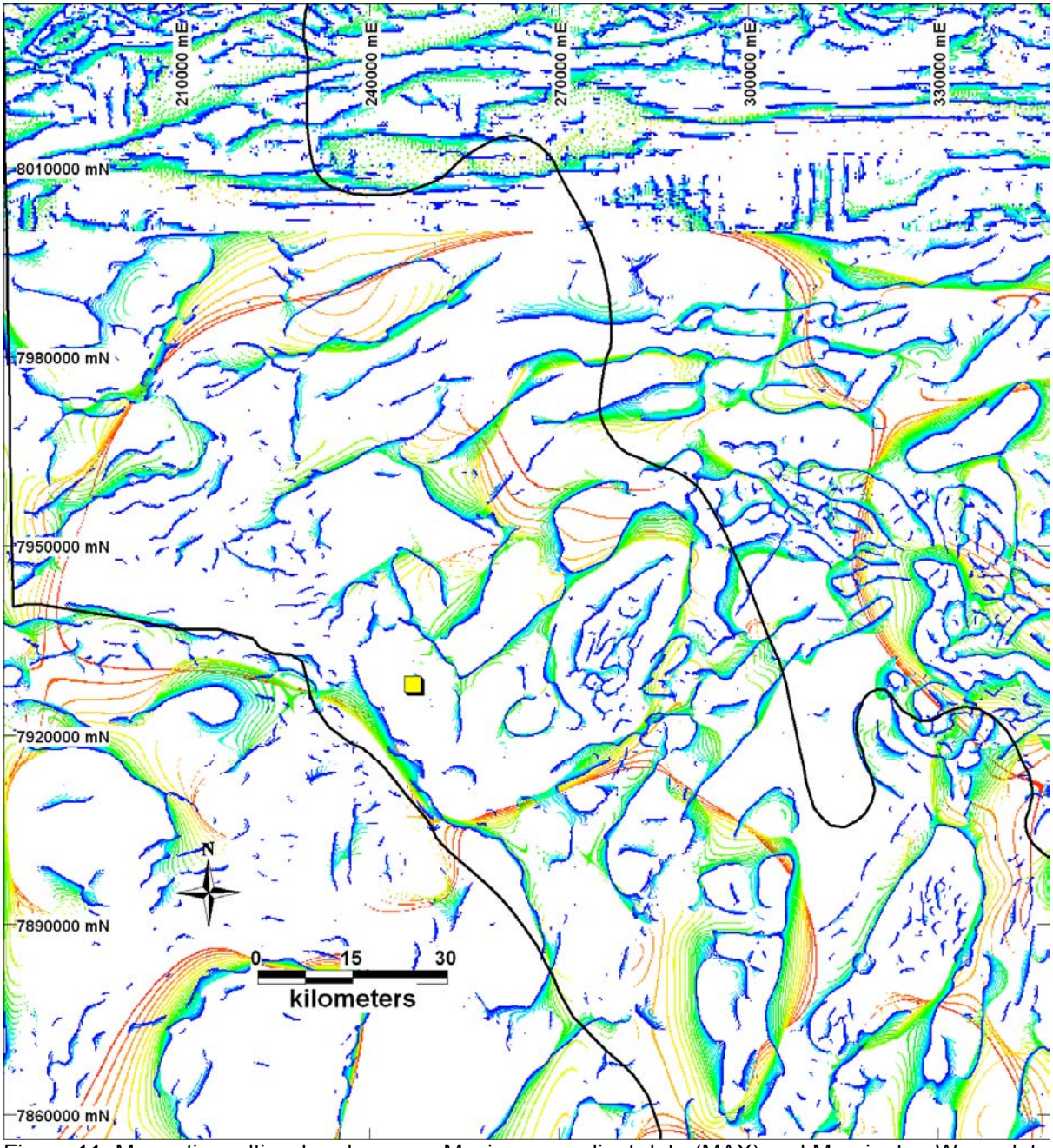

Figure 11: Magnetic multiscale edge map, Maximum gradient data (MAX) and Mornington Worm data (in northern region), coloured by height (Z) from 1km upward continuation (blue = fine scale, red/orange=coarse scale).

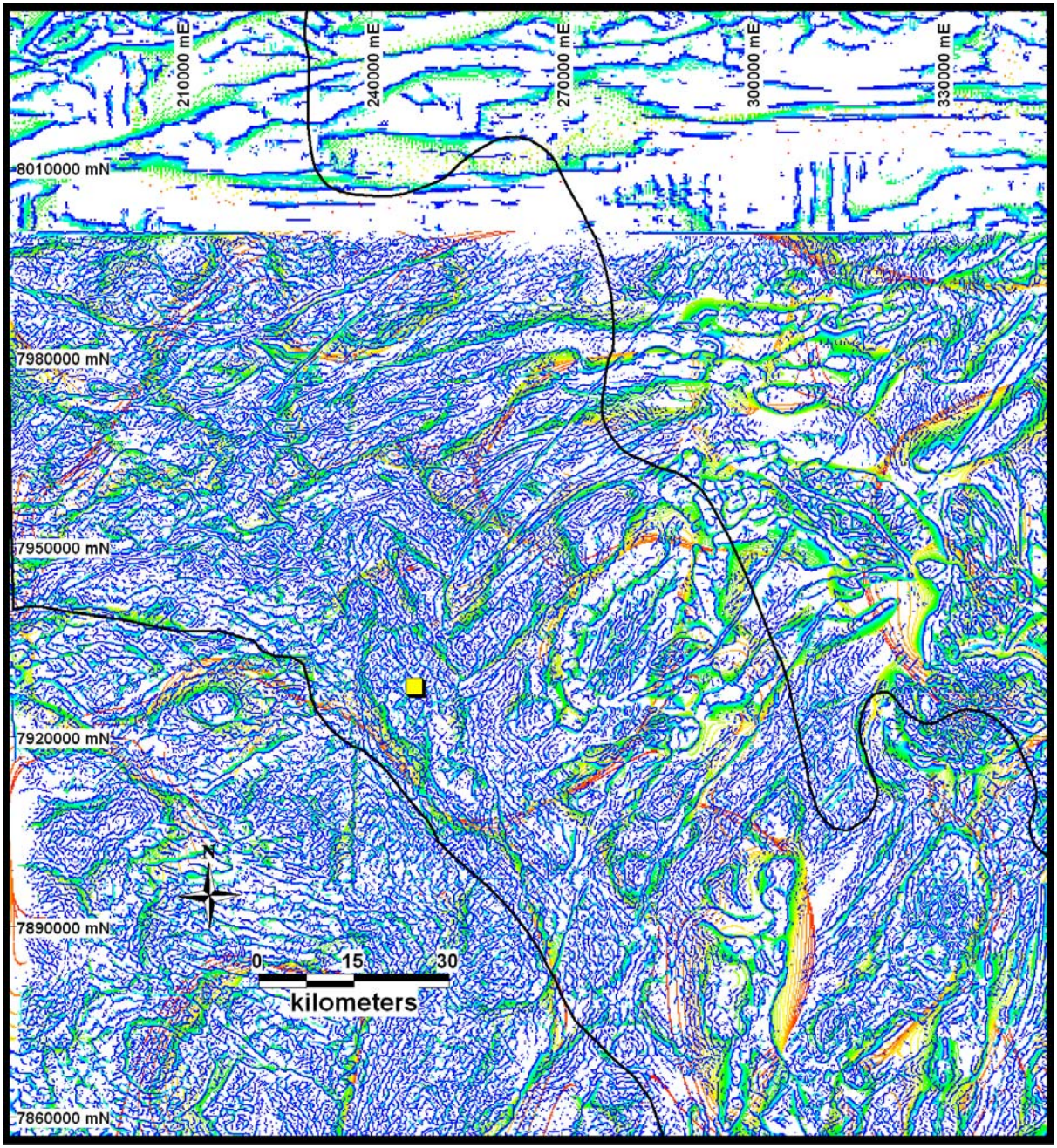

Figure 12: Magnetic multiscale edge map, Maximum gradient data (EFVD) and Mornington Worm data (in northern region), coloured by height (Z) from 1km upward continuation (blue = fine scale, red/orange=coarse scale).

5 Potential Field Gradient Interpretation

There is a broad coherence in the distribution of the gravity and aeromagnetic gradients. At a regional scale, similar linear trends are observed. For the purpose of this interpretation, a simple categorisation of line elements was made, based on whether the gradient encloses a coherent body (e.g. an intrusive) or if the gradient is “open” or linear in character. The latter features mostly relate to faults, dykes and stratigraphical contacts. A generalisation is that the majority of linear gradients are fault-related, however, this is consistent with the large population of faults in the outcropping region (Figure 6). These line elements are shown in Figures 13 and 14 for gravity and aeromagnetics respectively. The temporal superposition of the different orientations of fault elements has not been resolved here. The strike directions of the aeromagnetic fault lines are represented in Figure 15 showing that certain trends more prevalent within some areas. For example, the northern region is dominated by ENE gradients with long strike continuity. These are less well represented southwards

from about 7975000N where the NE trend is more evident. Further south and east the trend swings to NNE as, for example, along the Mt Gordon Fault. The NW trend, parallel to the Termite Range Fault, is well developed in the south-western region of the map (Figure 15).

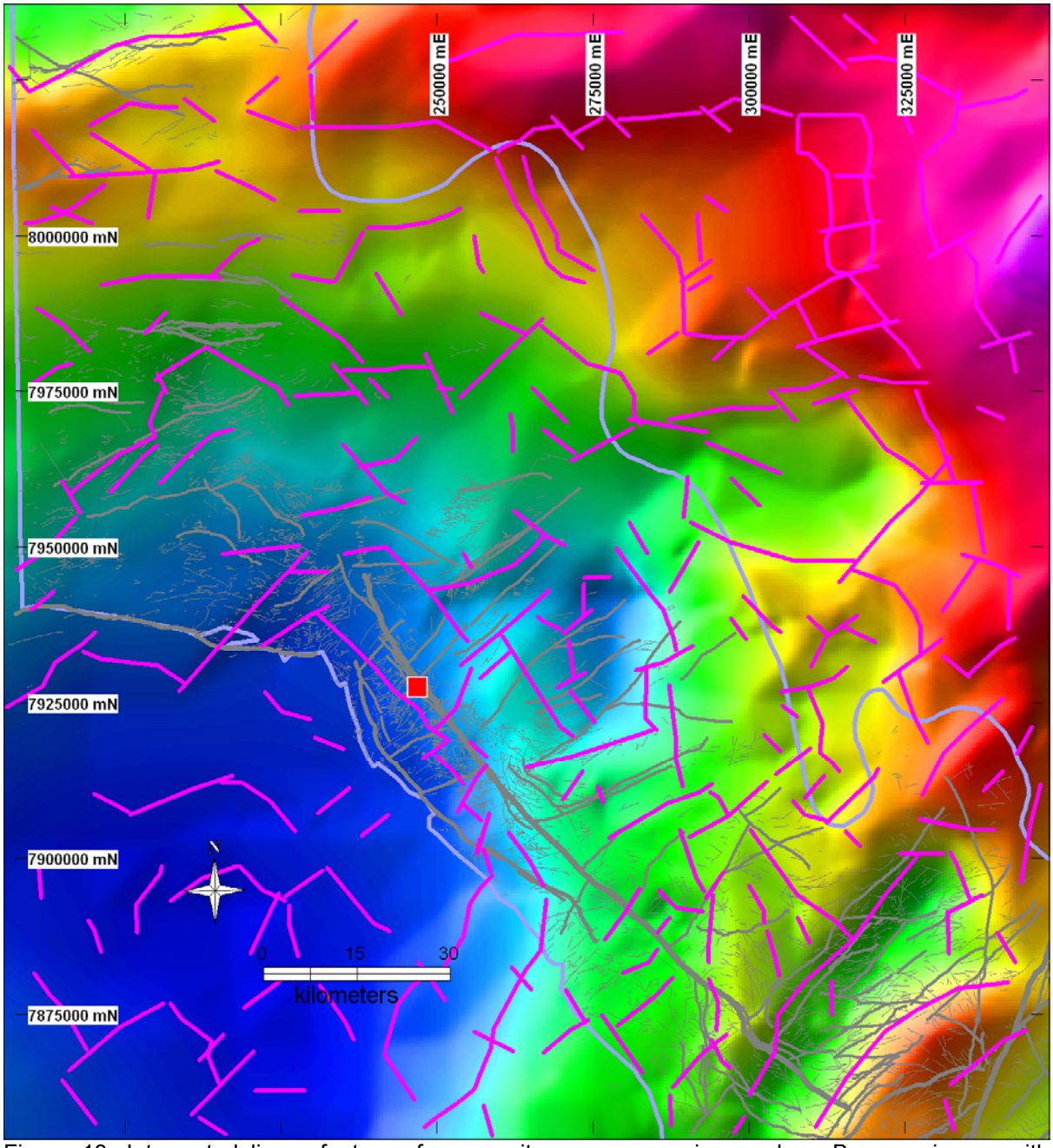

Figure 13: Interpreted linear features from gravity worms superimposed on Bouguer image with mapped faults (grey) and Century mine (red)

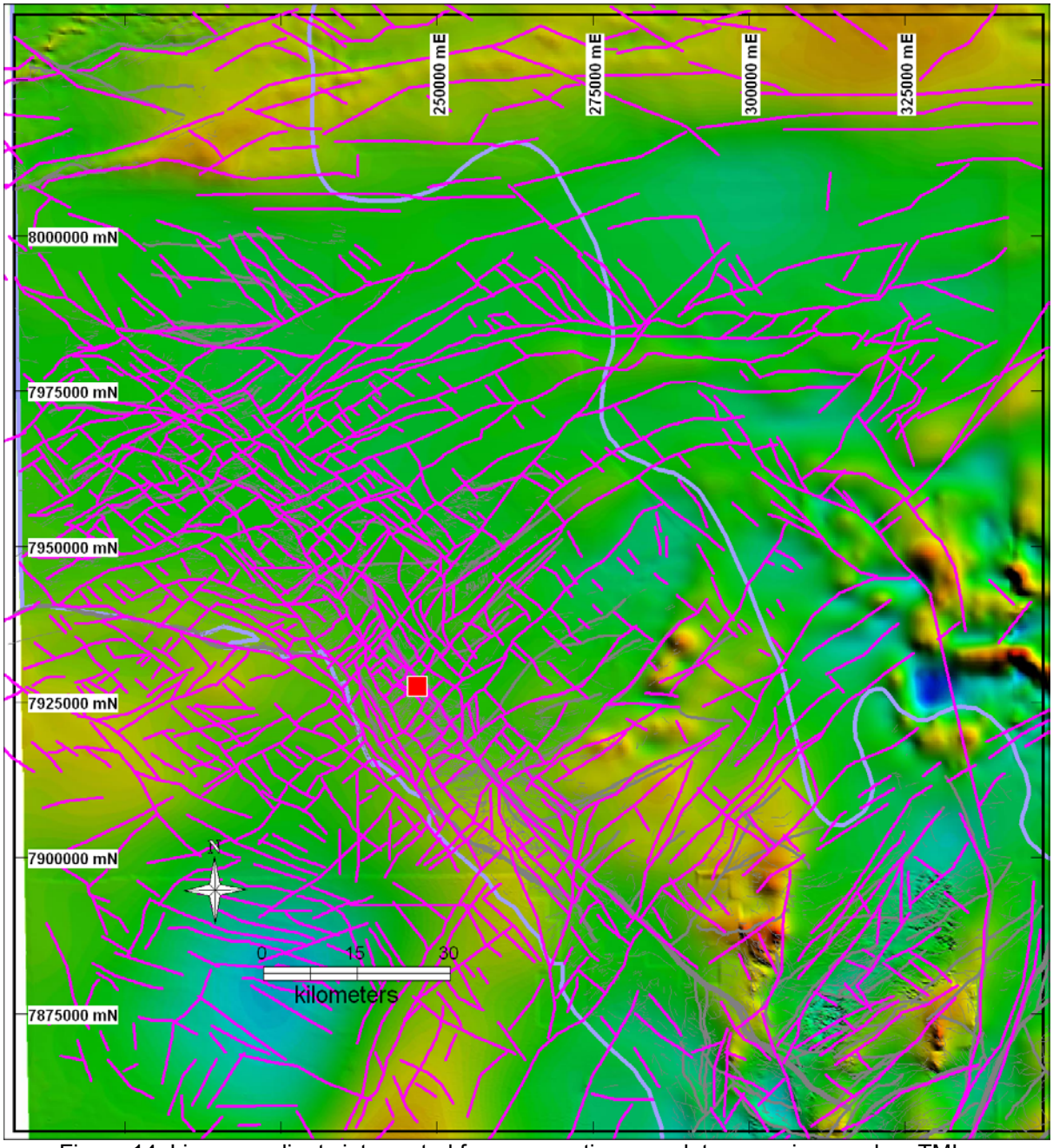

Figure 14: Linear gradients interpreted from magnetic worm data, superimposed on TMI.

Figure 15: Aeromagnetic Line interpretation coloured by average trend at 30^0 intervals.

Notwithstanding the inherent differences in the gravity and aeromagnetics, strike length is a key common attribute to both data sets. Length values may be extracted from the vector lines as a point file, gridded and imaged. This is shown for the aeromagnetics (Figure 16). The gravity line data is too sparse to generate a meaningful length grid. However the commonalities of the length values in both data sets allow an holistic view of the potential field gradients and to emphasise their coherence, rather than the individual differences, both gravity and aeromagnetic strike length data are combined and imaged (Figure 17). For completeness, these images also incorporate the length vales extracted from the mapped fault data (Figure 6). The relative intensities, rather than the absolute line lengths, are of value here for outlining the major fault architecture.

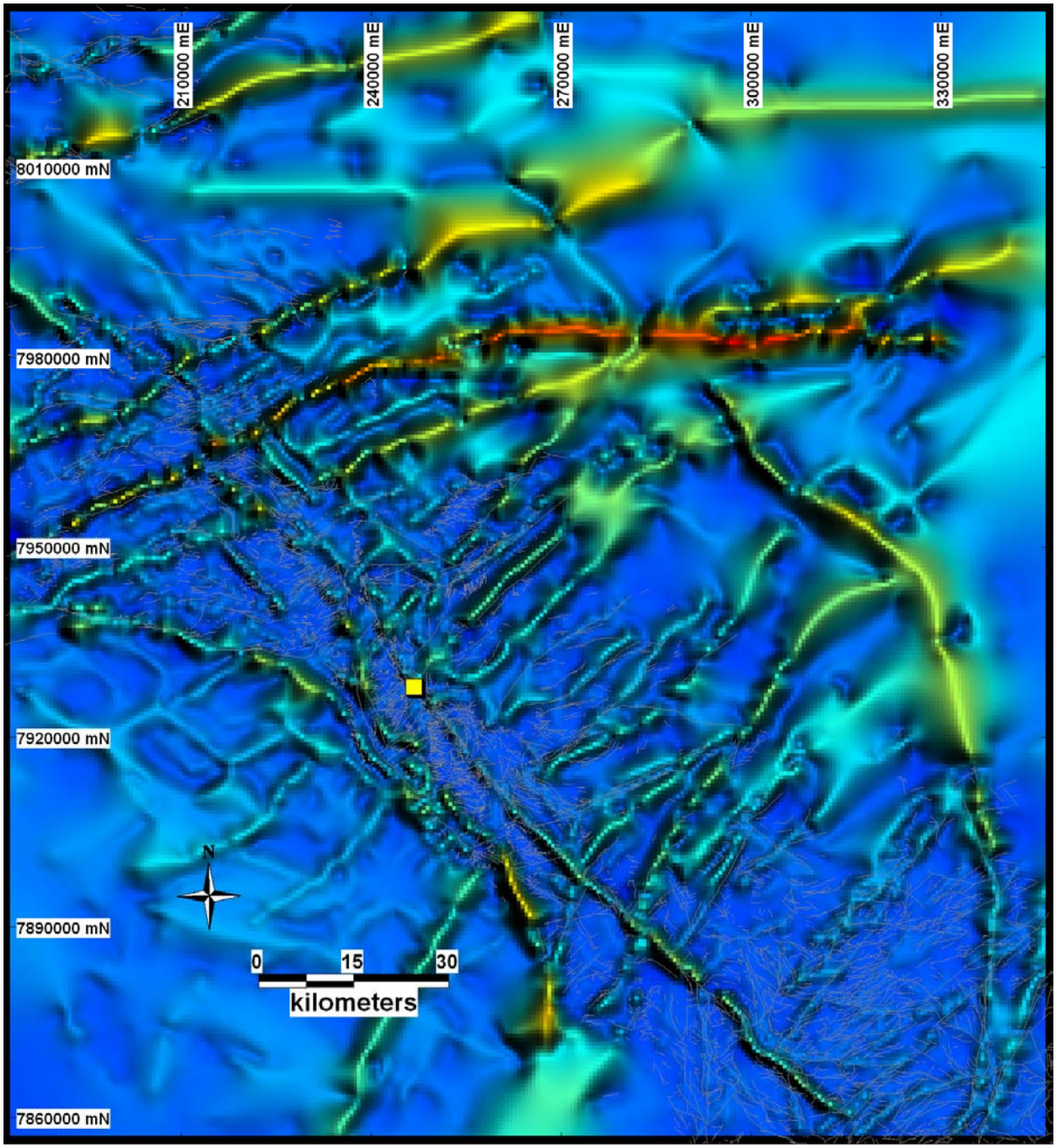

Figure 16: Line length image from interpreted linear gradients in aeromagnetics combined with mapped fault length values. – add Fault names

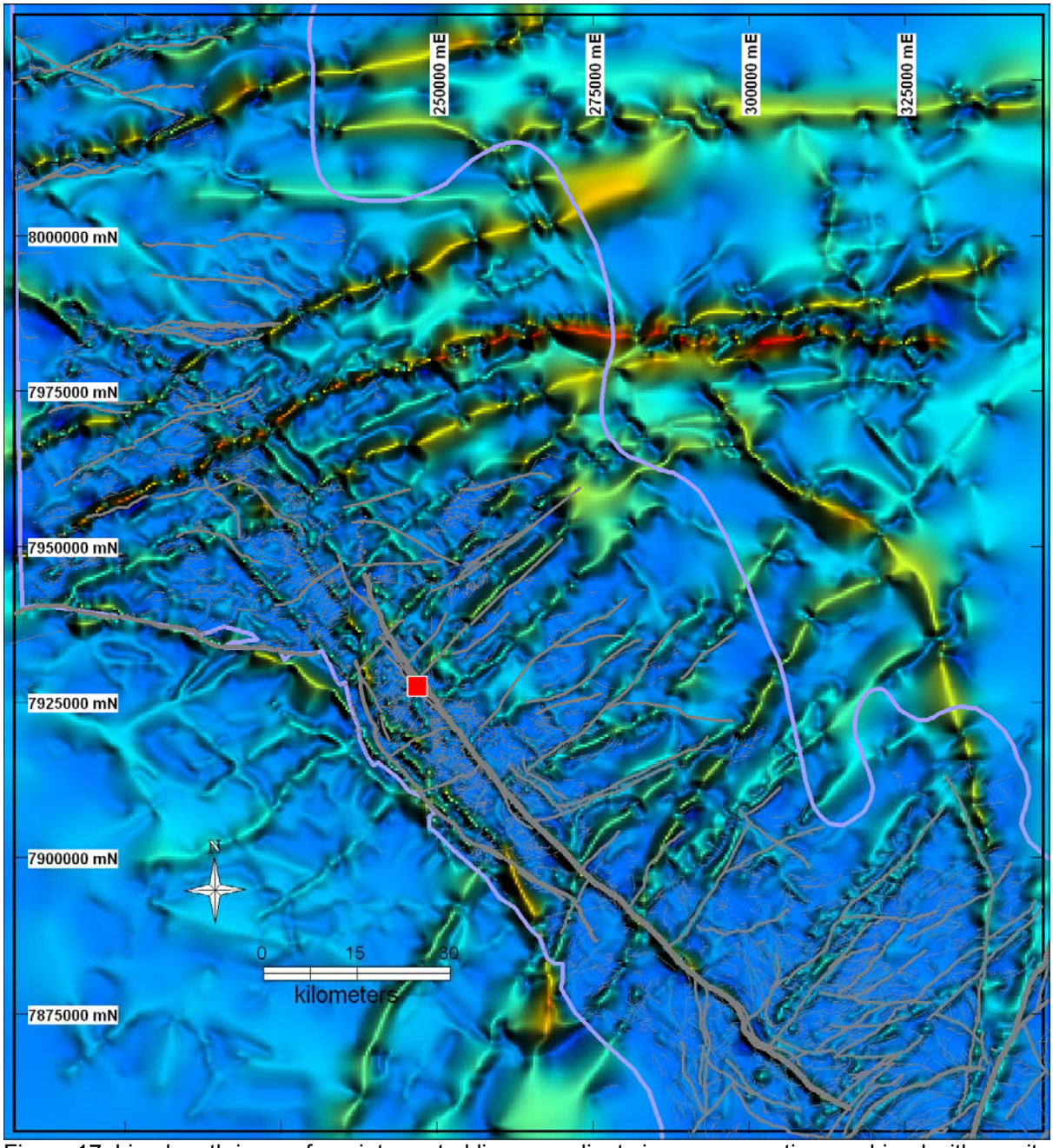

Figure 17: Line length image from interpreted linear gradients in aeromagnetics combined with gravity and mapped fault length values. – add Fault names

Not surprisingly, major faults are generally represented by long strike length features in these images. While the greatest uncertainty lies in the degree of connectivity inferred, it provides a reasonably robust regional structural template from which to build the 3D model. This type of analysis also serves to emphasis, in a more surprising way, the pattern of cross-faults, especially the sometimes enigmatic features that truncate worms. The inference is that at least some of these longer features have significant penetration, but are enigmatic as there is little density/susceptibility contract across them. The Termite Range and Riversleigh Fault corridor represent a major structural zone that cuts-across the regional NE trending features of the Lawn Hill Platform. While these NE elements are truncated, there degree of lateral offset is small, and a relative continuity of faults can be mapped across the Termite-Riversleigh Fault corridor. The northern extension of this corridor is more diffuse and segmented.

6 3D Geological Modelling

Together with the solid geology map (Figures 1 and 2) and the 2.5D interpretation of the fault-related features (e.g. Figure 17), the critical inputs to the 3D model are cross sections based on these data (Figure 5). Using cross sections and a geological base map, these data are then rendered in "3DWEG" space as points that record the geological entity (unit or fault), its dip and dip direction, and its relationship to underlying parts of the pile (e.g. conformable, on-lap, eroding). The positions and dips of major faults and their relative cross-cutting relationships (Table 2xx) were determined. As regional scale 3D modelling is computationally intensive, simplifications of boundaries were made particularly where complex or re-entrant shapes were encountered. Once built, the model was modified on the basis of subsequent information from magnetotelluric and seismic data, outlined below

Table 2: 3D Faults BEN

6.1 Cross Sections and Forward Modelling

Thickness estimates of units were captured from published sources (Sweet and Hutton, 1982; Figure 3) or estimated from the geological map and interpolated onto the lines of section. Existing geological sections were utilised, particularly those that derive from interpretation of the Westmoreland grid of seismic data (Figure 5; Scott *et al.* xxxx). Several iterations of the regional cross sections were made (e.g. Figure 18), involving more than one interpreter, until a final version was accepted for incorporation into the modelling program. The initial modelling from the cross sections was done without the benefit of new MT and seismic data acquired during the course of the project, but the 3DWEG program is flexible to making changes as required to generate new models.

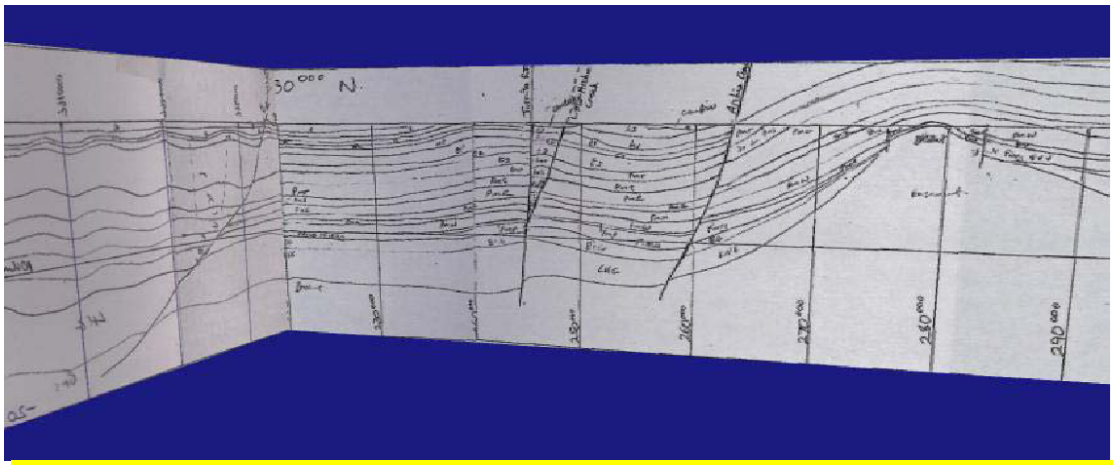

Figure 18: Example of two orientations of line drawn geological sections (7960000N and xxx) to 20 km depth.

Forward modelling of two N-S sections was undertaken to help constrain the interpretation (Figure 19). These parallel the two modelled sections in the AMIRA P552 project (Figure 20; P1 and P2, Scott *et al* ref). There are some significant differences in both sets of interpretations, however, particularly between P2 (Figure 20b) and 280000E (Figure 19b). The former has the major NE trending structures dipping southward whereas the preferred interpretation here is for northward dipping faults (similar to Betts *et al.* 2004). In both the P1 (Figure 20a) and 220000E sections (Figure 19a), the Little Range Fault is modelled as a major northward dipping boundary. This fault is interpreted to separate contrasting basement, with generally denser material at depth to the north (Figure 8). In the southern hanging wall of the fault there is a thinner development or an absence of Cover Sequence 1/Leichardt Superbasin equivalents and shallower pre-Barramundi basement (Murphy Metamorphics and inferred granites; see Figure 2). While there is uncertainty with this interpretation of the sub-Georgina Basin region, it is supported by the presence of the

Murphy Metamorphics to the west in the Carrara Range and by the newly acquired seismic to the west of Century.

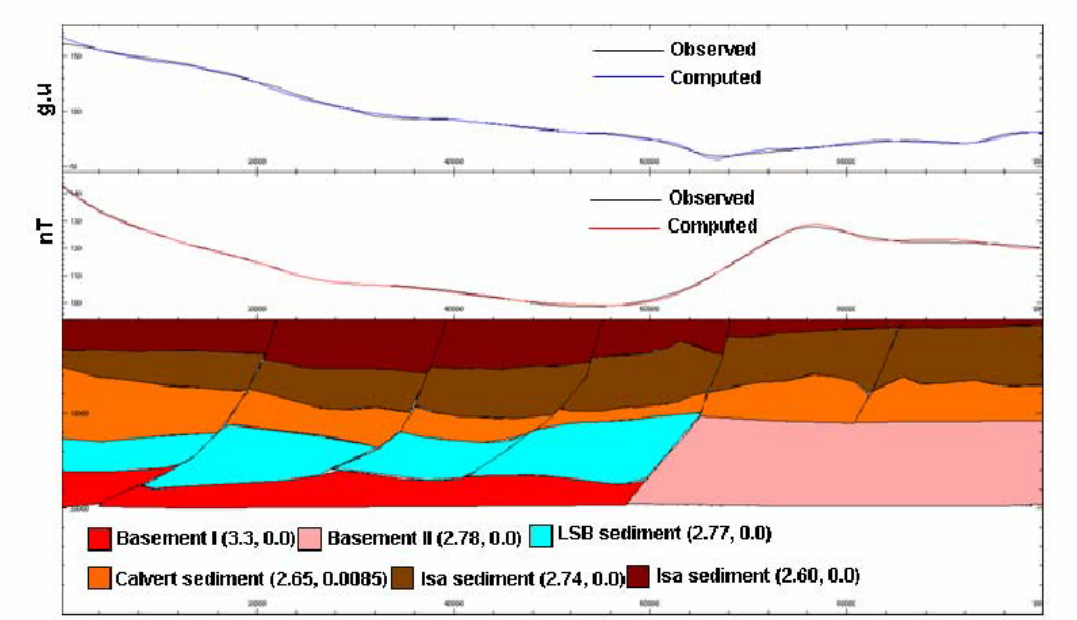

(a) N S

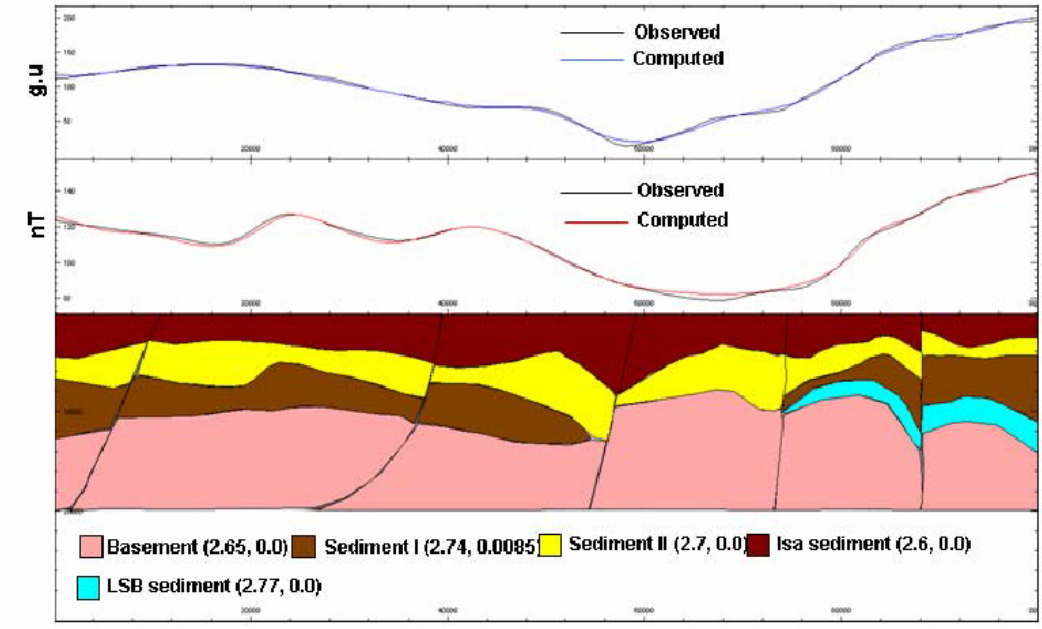

(b) N S

Figure 19: Forward modelled profiles on (a) 220000E and (b) 280000E lines, modelled to a depth of 20 km. See Figure 3 for locations of profiles.

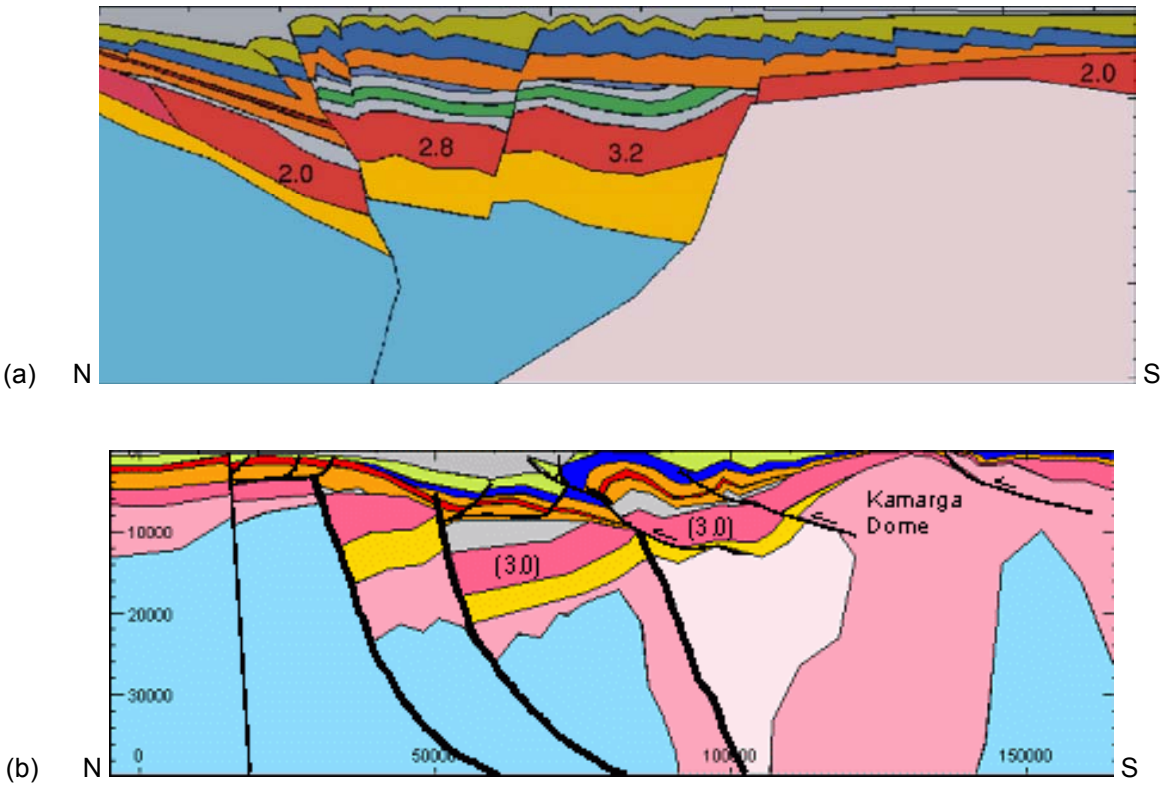

Figure 20: Forward modelled profiles from AMIRA P552 project (a) P1 and (b) P2 lines, modelled to a depth of 40 km (Scott *et al*. ref). See Figure 3 for locations of profiles.

6.2 Magnetotelluric Interpretation

Magnetotelluric (MT) soundings were obtained along two traverse lines to the north and west of the Century mine to investigate the nature of the Termite Range Fault (Murphy *et al*. in press). A preliminary interpretation of a 2D inversion profile (Figure 21) shows a more resistive, relatively flat lying, series of resistive/conductive layers in the top 5 km in the north western area that is truncated by a steep boundary. Projected to surface, this gradient change corresponds to the trace of the Termite Range Fault, with the inference that the fault itself extends to 10 km and perhaps to 20 km depth. The resistive/conductive layers are interpreted to lie in the hanging wall of the steep east dipping TRF. Upper layers with the 2D resistivity inversion model are reasonably well correlated with lithological units in this region, becoming more uncertain with depth In the south western footwall of the TRF, the resistive/conductive layers are much less evident. A second major fault, the Riversleigh Lineament (RL), is inferred from geology and gravity data and from a weak resistivity contrast in the MT data. This fault is interpreted as a buried structure, as distinct from the reactivated TRF. The two faults together may have created a wide damage zone (with an associated strike change) in the crust.

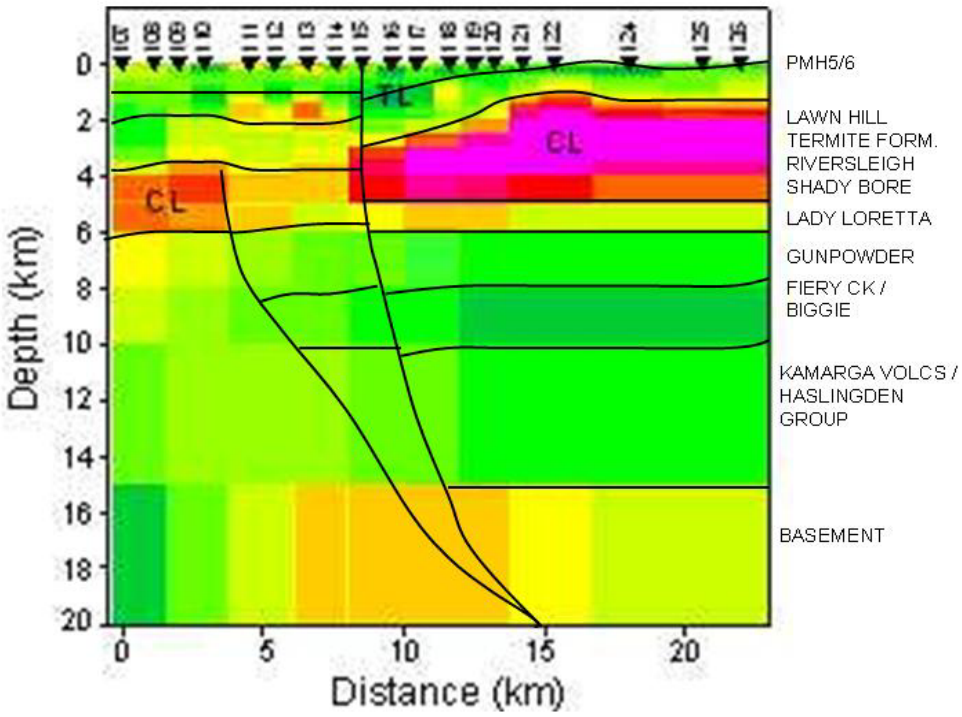

Figure 21: Interpreted geological boundaries on Magnetotelluric Line-1.

6.3 Seismic Interpretation

The Westmoreland grid was, up to recently, the only seismic data in the region and this provides key constraints relating to the southern margin of the Murphy inlier (Figure 4). Two newly acquired lines in the Century district (Figure 5) have successfully imaged a number of prominent reflectors and fault-related boundaries. A preliminary interpretation of these was made in a workshop with Geoscience Australia and the Geological Survey of Queensland, and further interpretation is required to derive a robust result. The first pass line interpretations, however, provide some key insights to the architecture. Significant faults from the seismic interpretation (Figure 22) are overlain on the MT profile. This has led to modifications being made to the 3DWEG program, from which a revised model was rendered:

- The Termite Range Fault appears to shallow at about 8 km depth, rather than being as steep as it is portrayed in the MT.
- the Riversleigh Fault is a major east dipping structure, shallower than previously modelled. It has an inferred growth fault history during Calvert Superbasin (CSB), as seen by increased thickness of these units in the seismic, compared to that previously inferred from the geological cross sections.
- the less reflective basement is at shallow levels to the west of the Riversleigh Fault, as suggested by the forward modelling and by the outcropping basement in the Northern Territory to the west.
- the basement level rises eastwards from the Termite Range Fault, consistent with exposure of older rocks in the nearby Kamarga Dome, and there is a draping of younger sedimentary units over this, in a similar fashion as depicted in the geological cross section (Figure 16). The top of basement in the hanging wall of the TRF is higher, at about 10 km, than was previously interpreted on the MT (at 14 km).

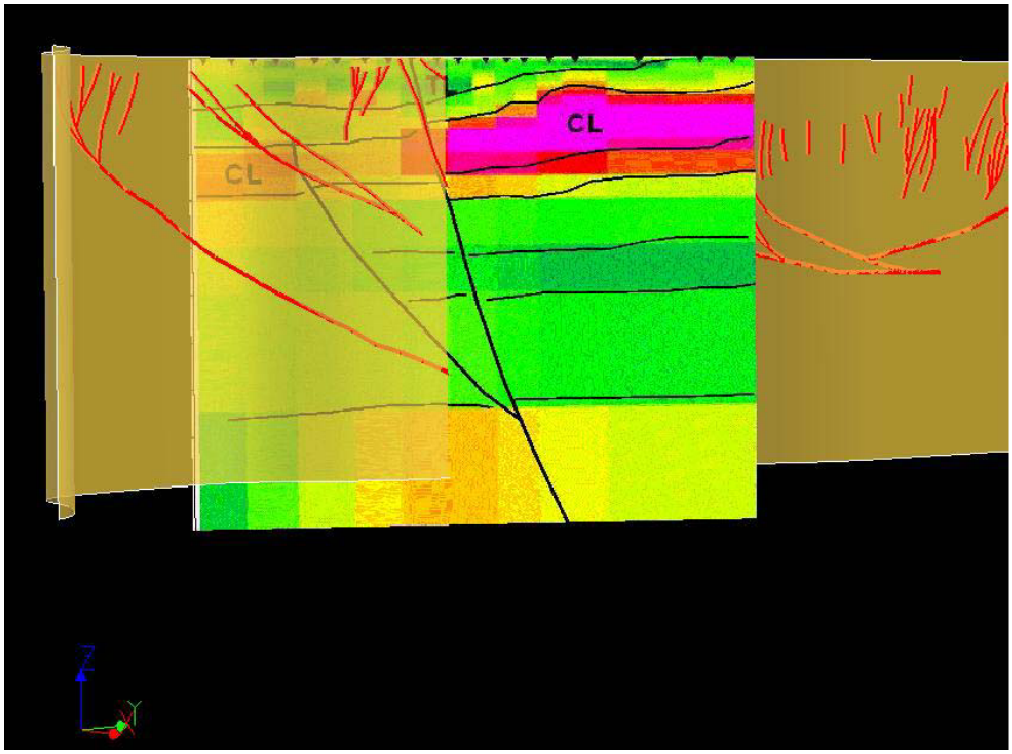

Figure 22: Perspective view of Interpreted faults (red lines) from seismic profiles and the MT inversion profile with previous interpretation (black lines).

6.4 3D Architecture

Aspects of the 3D model are illustrated here as a series of snapshots of its various components and geometries.

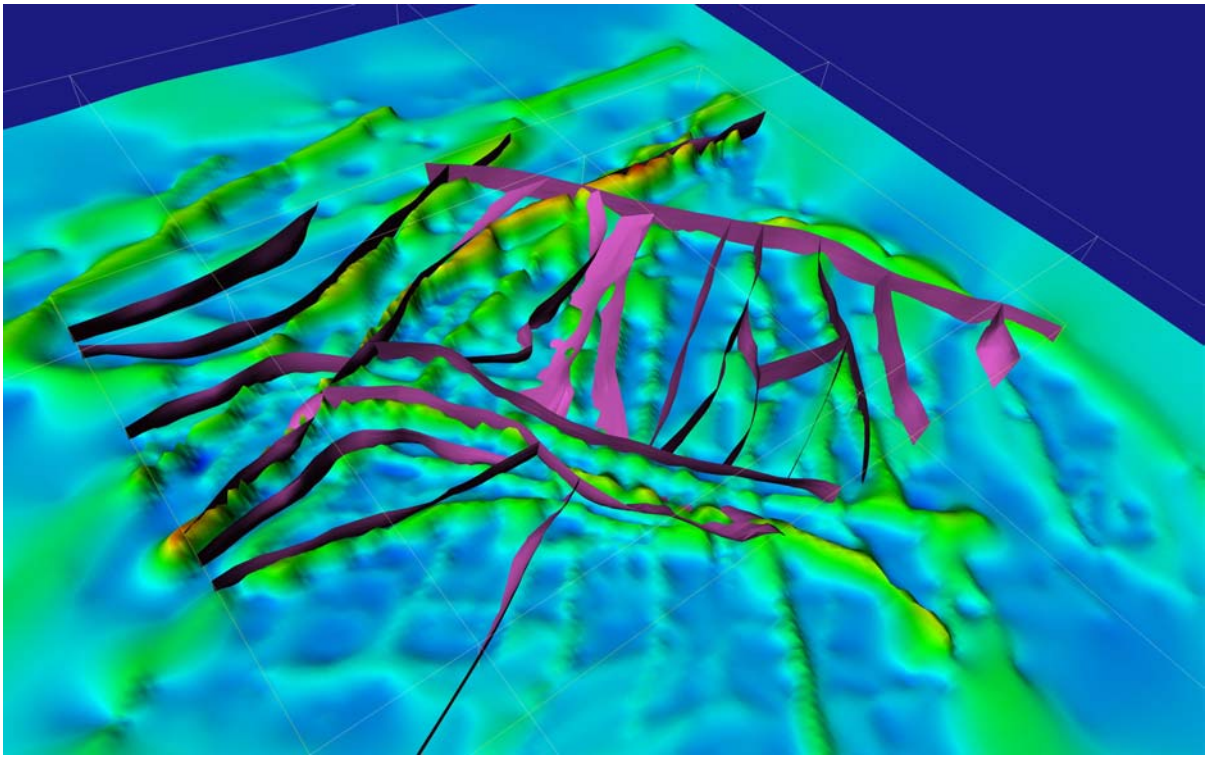

Figure 23: 3D modelled faults superimposed on magnetic line length image, view from west.

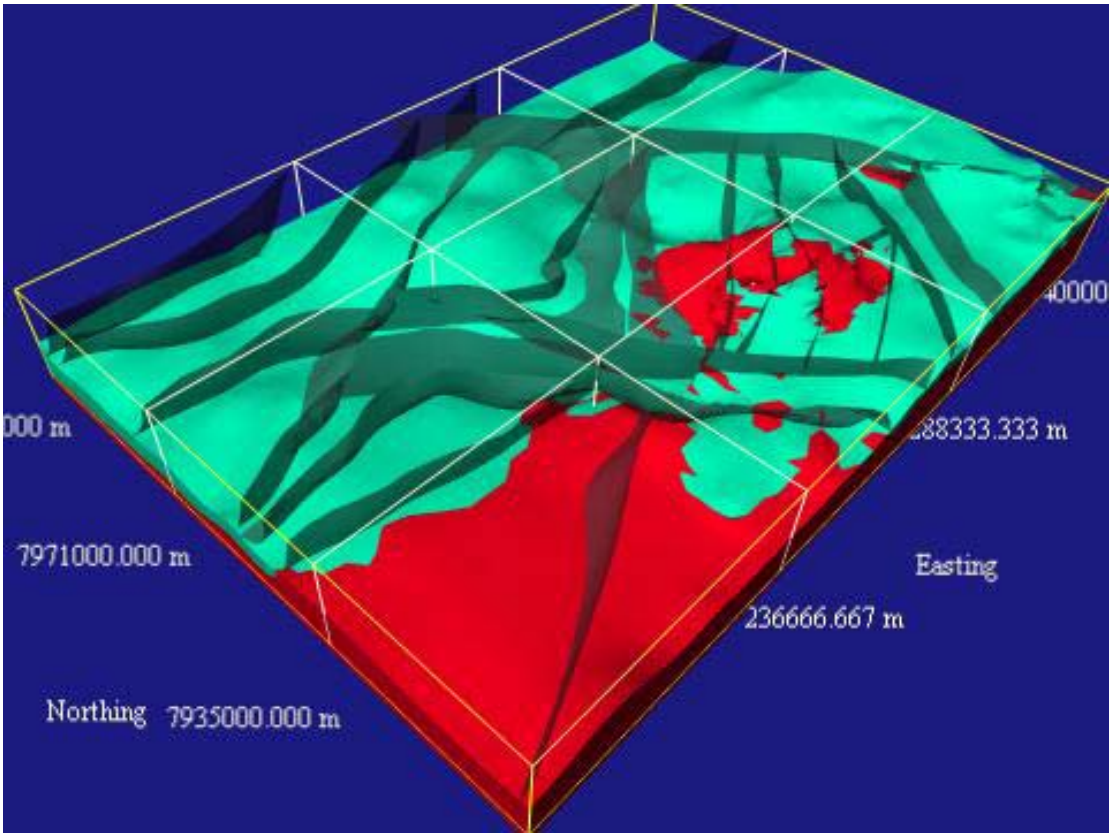

Figure 24: 3D model of basement (red), Leichhardt Superbasin (green) and modelled faults (grey), view from SW.

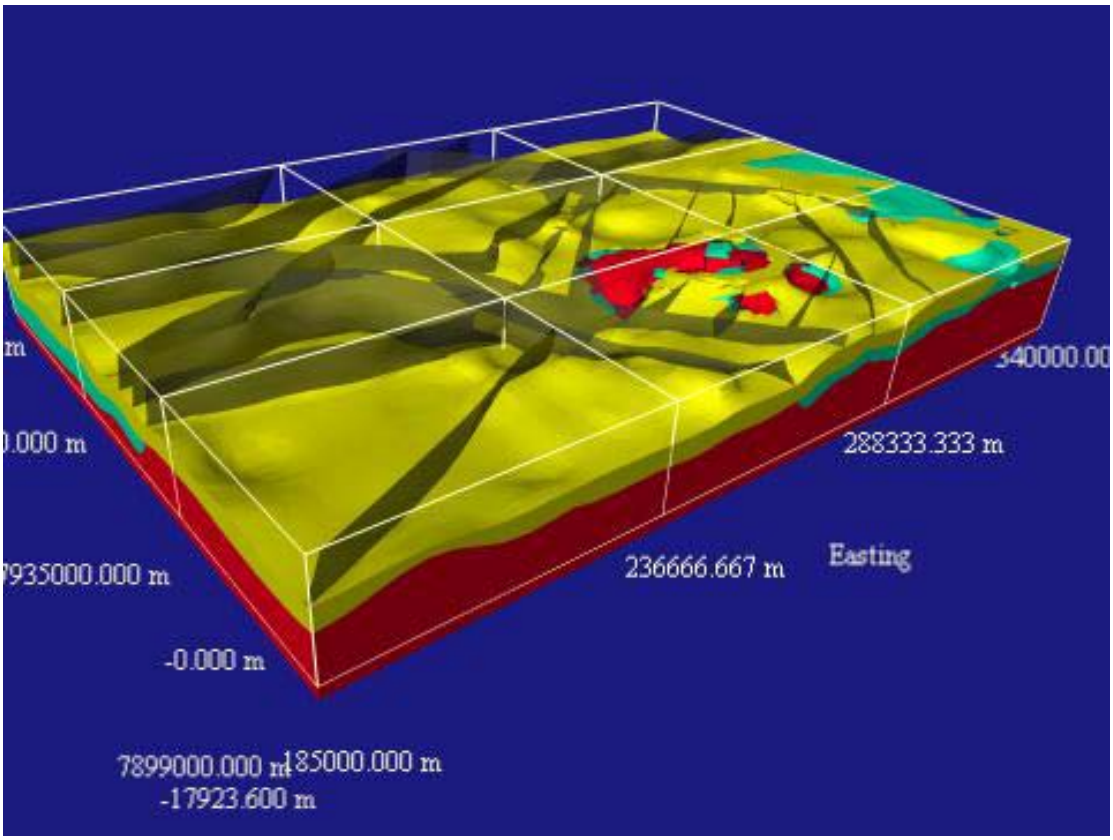

Figure 25: 3D model of basement (red), Leichhardt Superbasin (green) and Biggie (yellow; CSB) with modelled faults (grey), view from SW.

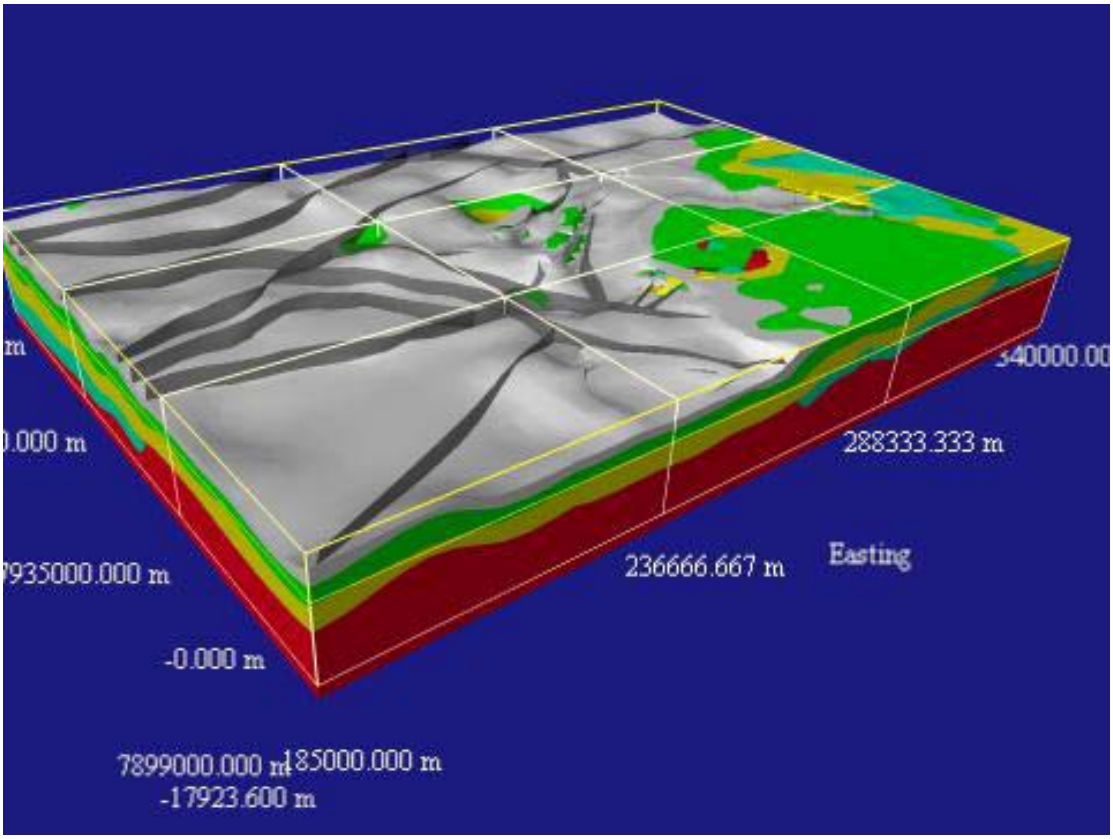

Figure 26: 3D model of basement (red), Leichhardt Superbasin (green) and Biggie (yellow), Torpedo Creek (green) and Shady Bore Quartzite (light grey) with modelled faults (grey), view from SW.

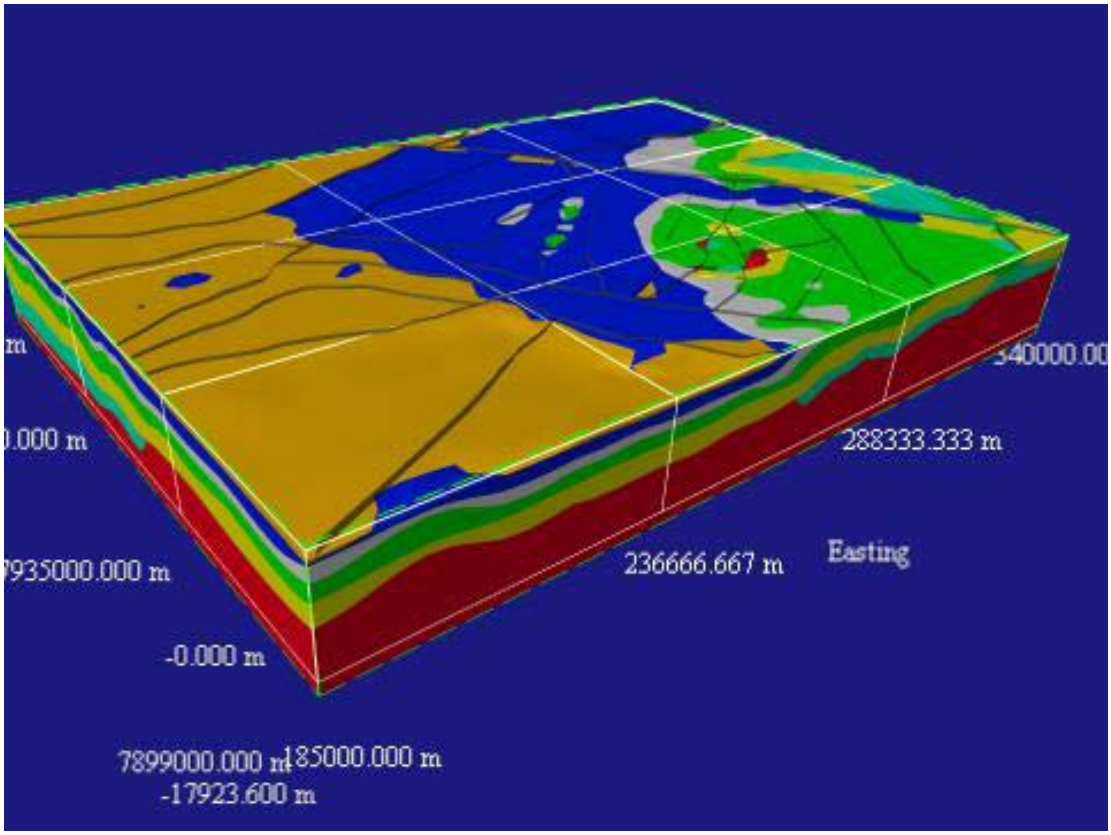

Figure 27: 3D model of basement (red), Leichhardt Superbasin (green) and Biggie (yellow), Torpedo Creek (green) and Shady Bore Quartzite (light grey), Termite Range Formation (blue) and South Nicholson Group (brown) with modelled faults (grey), view from SW.

7 Exploration Targeting

The localisation of the Century deposit close to a major fault intersection is a key factor in the numerical exploration models evaluated by Zhang *et al.* (2007). Applying the numerical outputs of the CSIRO-generated models for dilation and fluid flux into the spatial domain is a major challenge, as the spatial data is limited to strike length and trend. In order to constrain the distribution of fault intersections types, the aeromagnetic fault lines were evaluated (Figure 15) from which an intersection line length image derived (Figure 28). The large population of intersections have been attributed with intersecting line length and trend values. It is notable that the Century deposit is located in a relative "hot" spot intersection (Figure 28), just one of several similar intensity intersections along the Termite Range/Riversleigh Fault corridor.

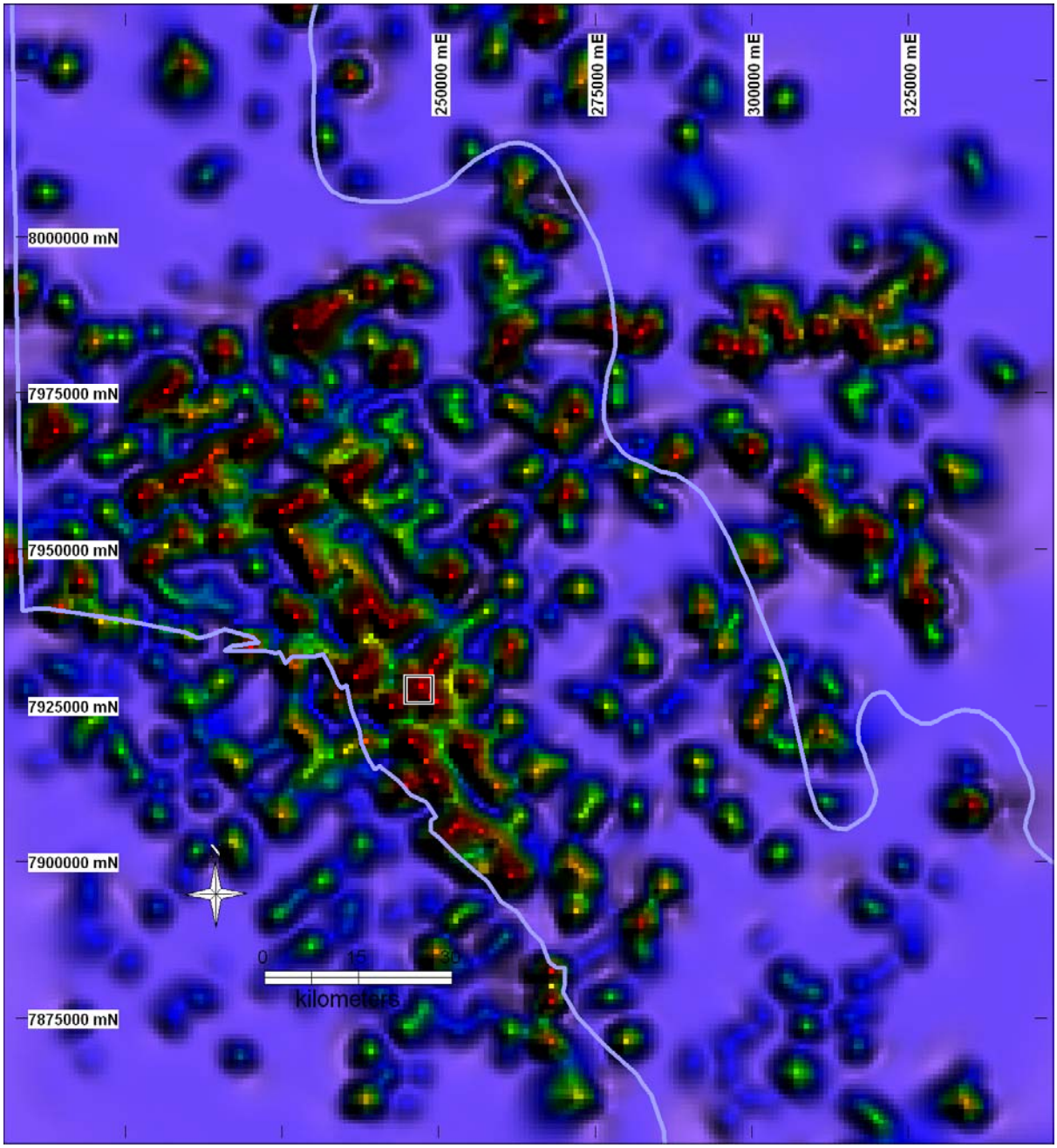

Figure 28: Intersection length-weighted image based on aeromagnetic fault-line interpretation. Warmer colours represent longer line intersections. Includes Proterozoic outcrop boundary and Century mine.

This data was captured using buffers (700m radius) on the intersection points and parameters visualised in Datadesk. Point values for the lines that occupy the buffer areas were extracted. The resulting intersection population ranges through maximum and minimum length and maximum and minimum trend distributions, shown respectively in Figure 29, colour coded here into three arbitrary groups. Intersections exceeding a maximum length of 80,000 m and a minimum length of 50,000 m (Figure 29a) are represented as the red and blue points, as distinct from the background population in black. The Century intersection region is contained in this grouping. These same points are shown in Figure 29b according to the minimum and maximum trend values. The blue points (including Century) are distinguished from the red points on the basis of different associated trends. The spatial distribution of these points is shown in Figure 29c, with the blue ones occupying the Termite Range/Riversleigh Fault corridor, and the red ones more so related to ENE structures in the LHP to the north. The population of blue coded intersections may be more favourably oriented with respect to the regional stress field, leading to higher dilation and fluid flux (check with Zhang).

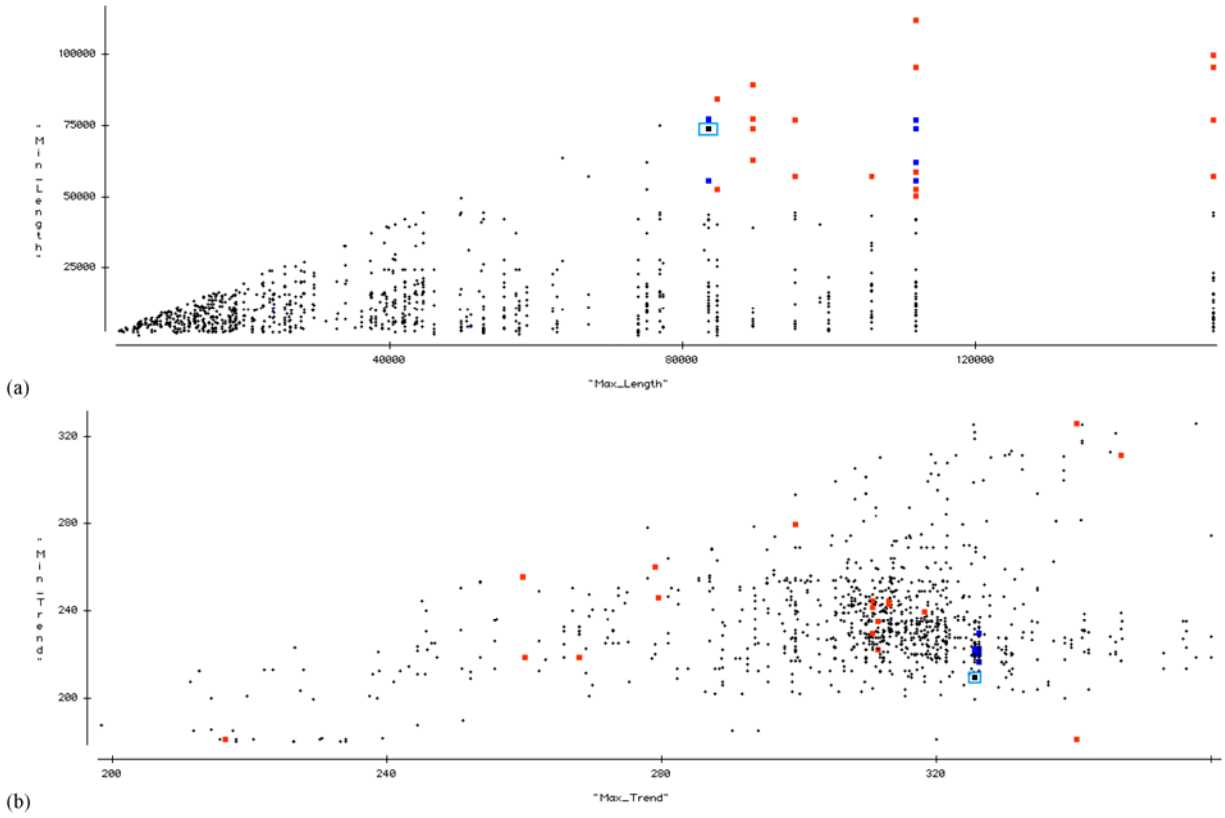

(c)

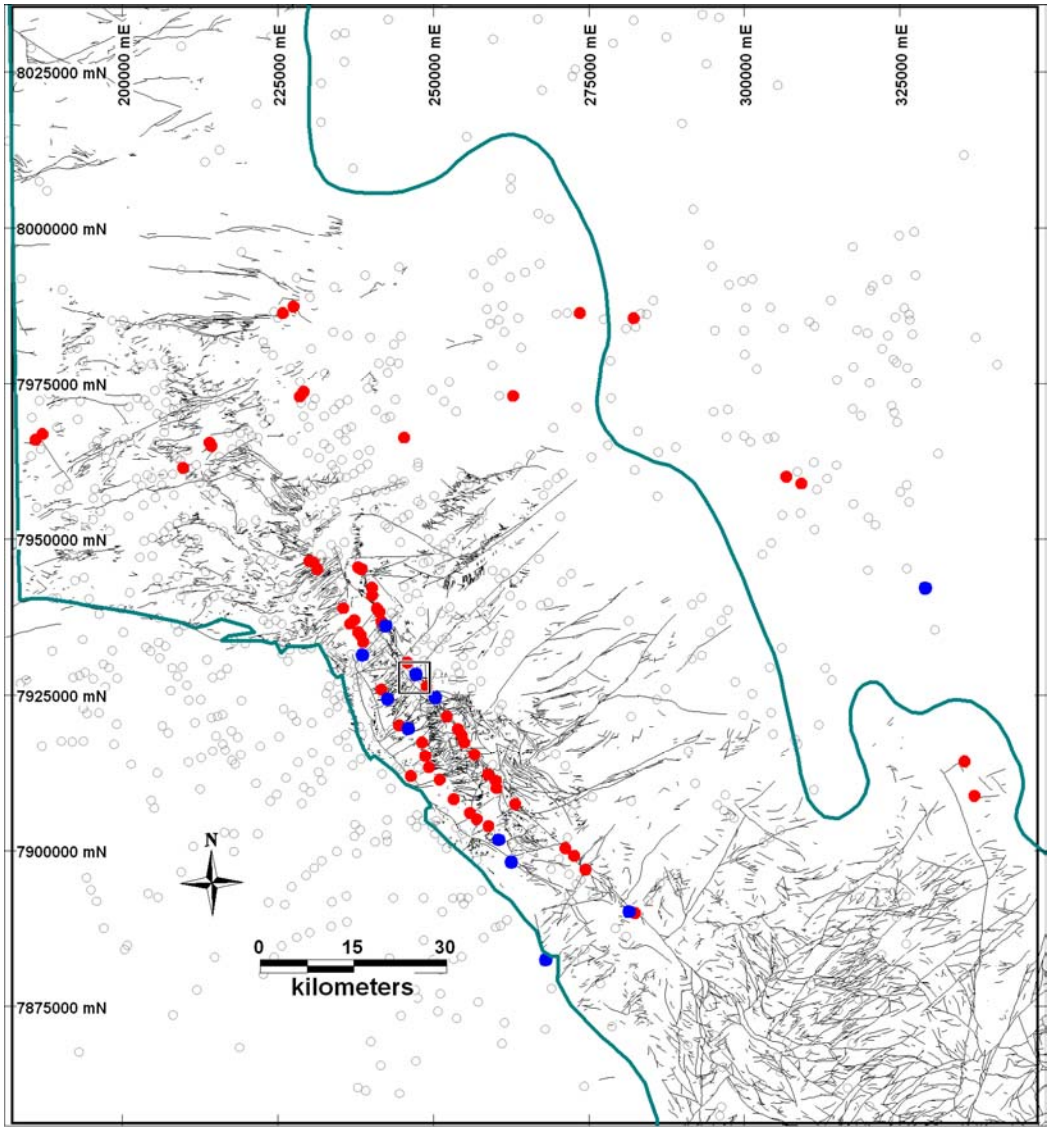

Figure 29: Aeromagnetic fault-line intersections as scatterplots of (a) Minimum and Maximum Length, (b) Minimum and Maximum Trend, and (c) spatial distribution of the population. See text for discussion of colour coding. Century deposit highlighted as boxed symbol in each plot.

An aeromagnetic signature associated with the Century deposit is seen in the EVFD worm data as an enigmatic ovoid feature (Figure 30). Its near coincidence with the deposit is considered significant, as a potential indicator of alteration, perhaps reflecting remnant magnetism in siderite alteration that characterises the ore system. If so, this style of feature may provide a direct targeting indicator as there are other similar features in the data. It was not possible to isolate these "blob-like" signatures quantitatively in the regional data (Figure 12), so the majority were manually traced. There is a significant variation in size and relative intensity of these enclosed gradients. Many of the larger shapes trace out domal fold patterns, as seen in the regional geology maps. Of the smaller Century-related signatures, however, there are several possibly similar areas, particularly to the NW of Century. A map of the main Termite Range/Riversleigh Fault corridor shows the location of these enclosed targets in relation to the intersection-related targets, geology and mineral occurrences (Figure 31). Variably overlapping relationships are seen, most notably at Century, but also in some other locations along the Termite Range/Riversleigh Fault corridor.

A 3D perspective of these data in relation to modelled faults and South Nicholson Group cover is shown as an example of possible targeting routines that can be applied (Figure 32).

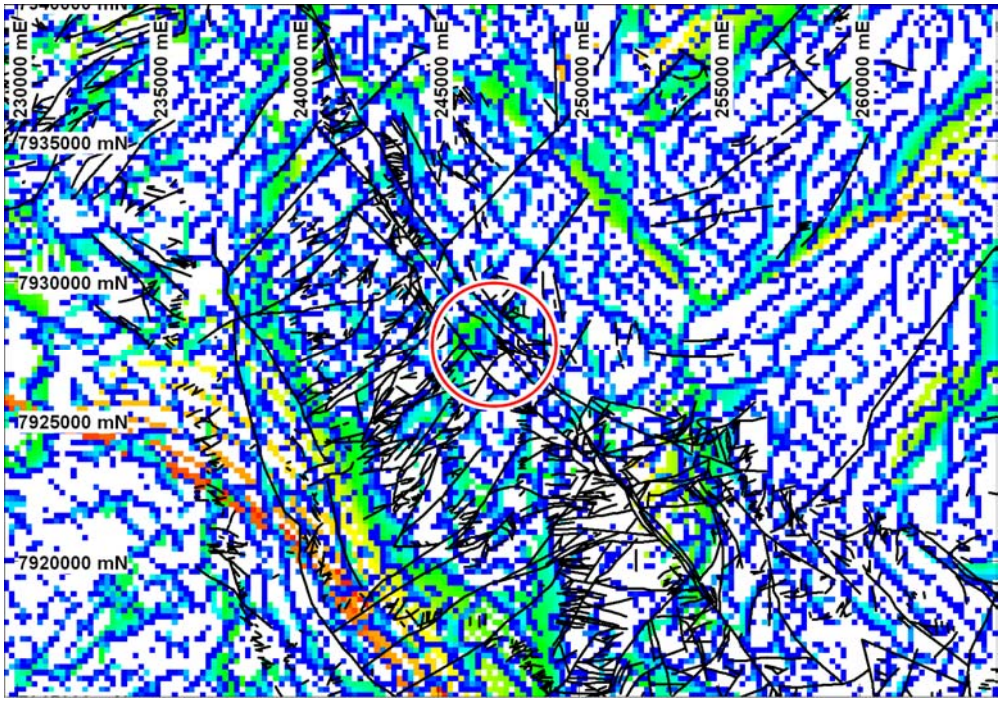

Figure 30: Aeromagnetic EFVD gradients coloured by upward continued height, mapped faults (black) and Century mine (circled). Note enclosed gradient signature in vicinity of Century deposit.

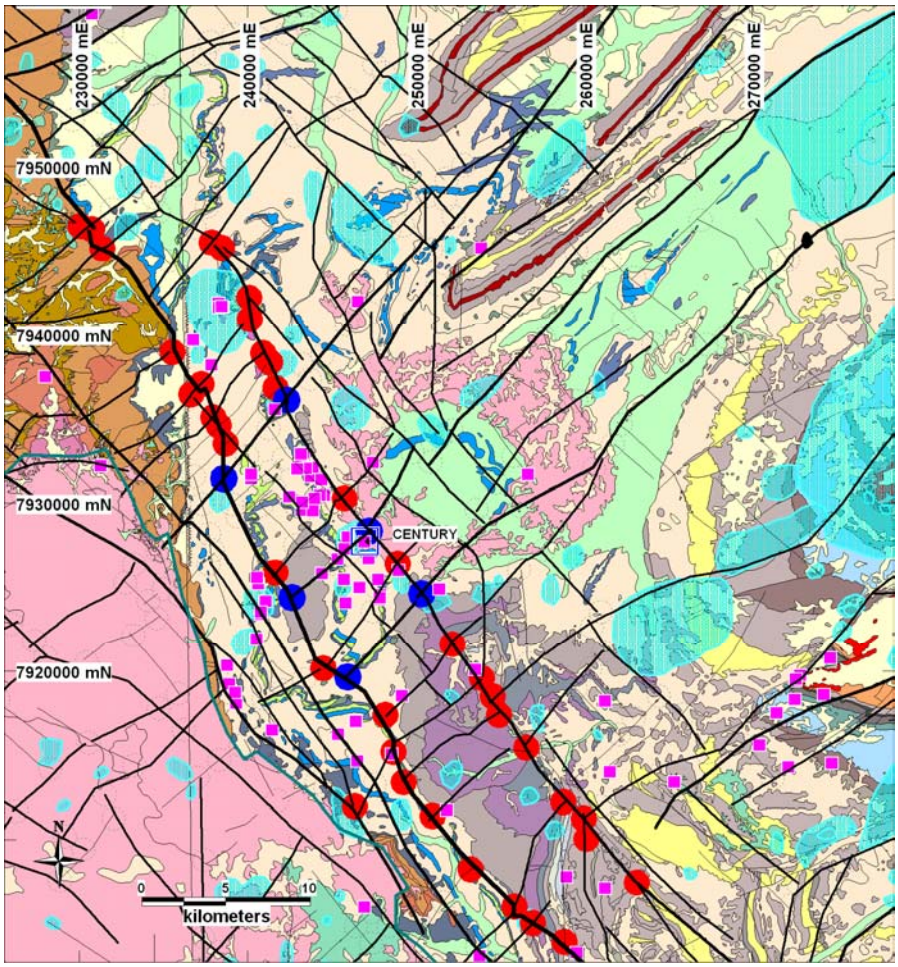

Figure 31: Termite Range/Riversleigh Fault corridor with locations of selected magnetic fault-line intersections (colour coded as per Figure 29), enclosed magnetic gradients (blue) and mineral occurrences (magenta dots).

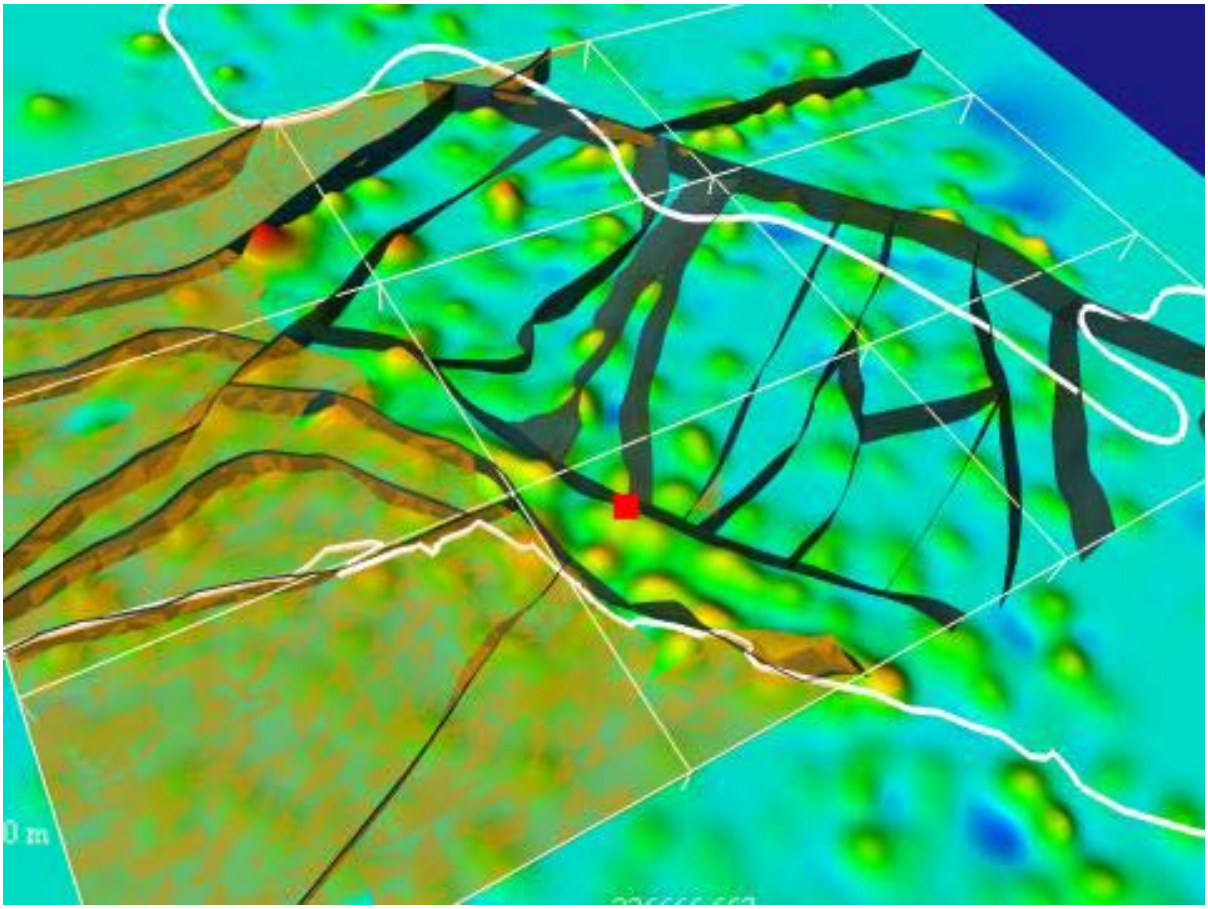

Figure 32: 3D faults superimposed on magnetic intersection length image, with overlay of South Nicholson Group (brown), Proterozoic outcrop boundary (white) and Century (red dot). Perspective view from SW.

8 Conclusions

Major fault boundaries are generally expressed as significant gradients in the aeromagnetic and/or gravity data. Multiscale wavelet processing (worms) helps to constrain the positions, orientations and depth extent of these gradients. In addition, this type of processing captures virtually all gradients which, through post-processing, make them amenable to thematic GIS treatments. The focus here is on linear, mostly fault-related gradients.

Strike length is a key attribute, common to faults, gravity and aeromagnetic gradients alike. Vectorised worm traces from gravity and aeromagnetic data were processed and length values extracted and imaged. It is apparent that many of the longer strike length features correlate with interpreted regional geological structures. In addition, the interpretation serves to highlight significant cross-faults of a scale and dimension that can be represented in regional 3D models.

…….to do

9 Acknowledgements

Input from Laurie Hutton (GSQ)

10 References

Archibald, N. J., Gow, P. and Boschetti, F. 1999. Multiscale edge analysis of potential field data. Exploration Geophysics, 30, 38-44.

Betts, P. G., Giles, D. and Lister, G. S. 2004. Aeromagnetic patterns of half-graben and basin inversion:implications for sediment-hosted massive sulphide Pb-Zn-Ag exploration. Journal of Structural Geology 26, 1137-1156.
Bierlein, F. P., Murphy, F. C., Weinberg R. F. and Lees, T. 2006. Distribution of Orogenic Gold Deposits in Relation to Fault Zones and Gravity Gradients: Targeting Tools Applied to the Eastern Goldfields, Yilgarn Craton, Western Australia. Mineralium Deposita, 41, 107-126.

Holden, D. J., Archibald, N. J., Boschetti, F. and Jessell, M. W. Inferring geological structures using multiscale edge analysis and forward models. Exploration Geophysics, 2000, 617-621.

Hornby, P., Boschetti, F. and Horowitz, F. 1999. Analysis of potential field data in the wavelet domain. Geophys. J. Internat. 137, 175-196.

Krassay, A. A., Bradshaw, B. E., Domagala, J., and Jaclson, M. J. 2000a. Siliciclastic shoreline to growth-faulted, turbiditic sub-basins: the Proterozoic River Supersequence of the upper McNamara Group on the Lawn Hill Platform, northern Australia. Australian Journal of Earth Sciences, 47, 533-562.

Krassay, A. A., Domagala, J., Bradshaw, B. E. and Southgate, P. N. 2000b. Lowstand ramps, fans and deep-water Palaeoproterozoic and Mesoproterozoic facies of the Lawn Hill Platform: the Term, Lawn, Wide and Doom Supersequences of the Isa Superbasin, northern Australia. Australian Journal of Earth Sciences, 47, 563-597.

Murphy, F. C. 2002. Structural framework and target generation in the Proterozoic Mt Isa region, Queensland, through analysis of potential field multiscale wavelets ("worms"). pmd*CRC report to MIM, available on Twiki web site)

Murphy, F. C. and Russell-Head, D., 2006. Characterisation of Potential Field Gradients using post-processed Multiscale wavelet edges. Abstract in Australian Earth Science Convention, Melbourne, p149.

Murphy, F. C. et al 2006 Victoria

Murphy, F. C, James Cull, J, Jong Lee, T., Kon Lee, S., and Song, Y. in press Magnetotelluric soundings and crustal architecture at Century Mine, Northern Australia. Australian Journal of Earth Sciences

Scott, D. L., Bradshaw, B. E. and Tarlowski, C. Z. 1998. The tectonostratigraphic history of the Proterozoic Northern Lawn Hill Platform, Australia: an integrated intracontinental basin analysis. Tectonophysics 300, 329-358.

Scott et al 2002?